PREDICTION BASED REAL TIME TRAFFIC MANAGEMENT USING CONNECTED AUTONOMOUS VEHICLES

by

Alperen Timuroğulları

B.S., Civil Engineering, Boğaziçi University, 2019

Submitted to the Institute for Graduate Studies in
Science and Engineering in partial fulfillment of
the requirements for the degree of
Master of Science

Graduate Program in Civil Engineering

Boğaziçi University

2021

ACKNOWLEDGEMENTS

First and foremost, I would like to express my special thanks, deepest gratitude, and respect to my advisor Assoc. Prof. Ilgın Gökaşar for her unwavering support and guidance, along with invaluable contributions throughout my time as her student. Thanks to her in-depth knowledge, comprehensive insights, and constant encouragement, I have been able to complete this study in a way that I get gratified and honored. Her vision, sincerity, and enthusiasm have made this an inspiring experience for me. It was a great privilege to work and study under her guidance.

I gratefully acknowledge that this project, with project number 15387 and project code 19A04R2, is conducted with the support of Boğaziçi University Research Fund. I am incredibly thankful for the opportunities that have come with this fellowship to further my research.

I am deeply indebted to my parents and sister as they have never wavered in their support, encouragement, and profound belief in my work and abilities and have always been there for me with their unconditional love all through my life.

I would also express my sincere gratitude to my girlfriend Tuğçe Akdöker as her unparalleled support and encouragement have aided me immensely and have kept my motivation and endeavors at the highest possible level.

Lastly, I would like to express my deepest appreciation to Sarp Semih Ozkan and Burak Altın for their invaluable contributions and sincere support all through my thesis.

ABSTRACT

PREDICTION BASED REAL TIME TRAFFIC MANAGEMENT USING CONNECTED AUTONOMOUS VEHICLES

The increasing population of big cities and hence the increasing rate of vehicle use with the population bring important environmental and economic problems. Traffic congestion is one of the main causes of these problems. The presence of factors that may cause traffic to slow down or even stop locally increases the density of traffic, especially in highly populated cities, and the effect of these factors can cease to be local and affect the entire road network. Therefore, the effective management of traffic plays an essential role in reducing these negative effects. In this thesis, the real-time management using the connected autonomous vehicles, namely SWSCAV, [1] was tested in the 11 km long road network using the SUMO (Simulation of Urban Mobility) environment. Then, SWSCAV [1] with and without the prediction was compared with two real-time traffic management methods, namely the Variable Speed Limits and Lane Control Systems. 2400 different scenarios were created changing the parameters: the control distance and the percentage of the connected autonomous vehicles in the traffic flow. SWSCAV [1] with prediction where there are 50% connected autonomous vehicles decreased the density by an average of 58.18%. This scenario provided a 61.61% decrease in the density locally with a control distance of 1250 meters.

ÖZET

BAĞLI OTONOM ARAÇLARI KULLANARAK TAHMİNE DAYALI GERÇEK ZAMANLI TRAFİK YÖNETİMİ

Büyük şehirlerin artan nüfusu ve dolayısıyla nüfusla birlikte artan araç kullanım oranı, önemli çevresel ve ekonomik sorunları da beraberinde getirmektedir. Trafik sıkışıklığı, bu sorunların ana nedenlerinden biridir. Trafiğin yavaşlamasına ve hatta yerel olarak durmasına neden olabilecek faktörlerin varlığı, özellikle yüksek nüfuslu şehirlerde trafik yoğunluğunu arttırır ve bu faktörlerin etkisi yerel olmaktan çıkıp tüm yol ağını etkileyebilir. Bu nedenle, trafiğin etkin yönetimi, bu olumsuz etkilerin azaltılmasında önemli bir rol oynar. Bu tezde, SWSCAV [1] adı verilen bağlı otonom araçları kullanan gerçek zamanlı trafik yönetimi yöntemi, SUMO (Simulation of Urban Mobility) ortamı kullanılarak 11 km uzunluğundaki yol ağında test edilmiştir. Daha sonra tahminli ve tahminsiz SWSCAV [1], Değişken Hız Sınırları ve Şerit Kontrol Sistemleri olmak üzere iki gerçek zamanlı trafik yönetimi yöntemi ile karşılaştırılmıştır. Kontrol mesafesi ve bağlı otonom araçların trafik akışındaki yüzdesi parametreleri değiştirerek 2400 farklı senaryo oluşturulmuştur. Trafikteki otonom araçların sayısının tüm araçlara oranının % 50 olduğu tahminli SWSCAV [1] yöntemi, kritik bölgedeki yoğunluğu ortalama% 58,18 azaltmıştır. Bu senaryo, 1250 metrelik bir kontrol mesafesinde yerel olarak yoğunlukta % 61,61 azalma sağlamıştır.

TABLE OF CONTENTS

ACKNOWLEDGEMENTS . . . iii
ABSTRACT . . . iv
ÖZET . . . v
LIST OF FIGURES . . . viii
LIST OF TABLES . . . xi
LIST OF SYMBOLS . . . xiii
LIST OF ACRONYMS/ABBREVIATIONS . . . xiv
1. INTRODUCTION . . . 1
1.1. Introduction and Motivation . . . 1
1.2. Autonomous Vehicle Studies in the Literature . . . 2
1.3. Traffic Management using CAVs in the Literature . . . 3
2. THEORY . . . 5
2.1. Shockwave . . . 5
2.2. Fast Fourier Transform (FFT) Upsampling . . . 6
2.3. Fused Lasso . . . 8
2.4. Pix2Pix Generative Adversarial Networks Algorithm . . . 9
3. METHODOLOGY . . . 12
3.1. Simulation of the Study Network using SUMO . . . 12
3.1.1. Assumptions of the Network . . . 15
3.1.2. Simulation Workflow . . . 15
3.1.3. Common Scenario Parameters . . . 15
3.1.4. Data Collection and Storage Process . . . 16
3.1.5. LCS Implementation . . . 18
3.1.6. VSL Implementation . . . 20
3.1.7. SWSCAV [1] Implementation . . . 22
3.1.7.1. Shockwave Detection . . . 24
3.1.7.2. Application of Data Up-sampling . . . 25
3.1.7.3. Application of Data Smoothing . . . 27

3.1.7.4. Shockwave Speed Calculation 27
3.1.8. SWSCAV with Prediction [1] Implementation 28
3.1.8.1. Training and Implementation of Pix2Pix Algorithm . . 30
3.1.9. Measures of Effectiveness 31
3.1.10. Heatmaps 40
3.1.11. Comparison with LCS and VSL 42
3.1.12. Simulation Results of Predicted Control Method 44
3.1.13. Lineplots 48
3.1.14. Heatmaps 52
3.1.15. Comparison of Predicted Control Method with LCS and VSL . 58
3.1.16. 3D Plots 68
4. CONCLUSION 71
REFERENCES 74

LIST OF FIGURES

Figure 2.1. Shockwave parameters at state A and state B 5

Figure 2.2. Fast Fourier Upsampling applied to the sample of traffic density data 8

Figure 2.3. Up-sampled traffic density data with Fused Lasso application . . . 9

Figure 2.4. Measured input density image(left-most), target density image(middle) and predicted density image(right-most) 11

Figure 3.1. Flow chart of the methodology. 12

Figure 3.2. The study network 13

Figure 3.3. Illustration of LCS Implementation on a 4-Lanes Road (TRUMM, 2010) 18

Figure 3.4. Sensors Locations 19

Figure 3.5. The flowchart of LCS implementation 20

Figure 3.6. The sketch of the study network for VSL implementation 21

Figure 3.7. VSL simulation flowchart 22

Figure 3.8. Flowchart of SWSCAV [1] Implementation 24

Figure 3.9. Shockwave Detection Algorithm 25

Figure 3.10. Average Density Values at Sensor Locations 26

Figure 3.11. Up-sampled Average Density Values at Sensor Locations 26

Figure 3.12. Smoothed Up-sampled Average Density Values at Sensor Locations 27

Figure 3.13. The flow chart of the implementation of SWSCAV with the prediction [1] 29

Figure 3.14. Illustration of Critical Region 34

Figure 3.15. Density vs Time at the Incident Location 39

Figure 3.16. Speed vs Time at the Incident Location 40

Figure 3.17. Uncontrolled Traffic Density Heatmap (seed=25) 41

Figure 3.18. Controlled Traffic Density Heatmap(seed=25, CD=1000m, PR=70%) 42

Figure 3.19. Time vs Density Graph 750m 48

Figure 3.20. Time vs Density Graph 1000m 48

Figure 3.21. Time vs Density Graph 1250m 49

Figure 3.22. Time vs Speed Graph 750m 50

Figure 3.23. Time vs Speed Graph 1000m 50

Figure 3.24. Time vs Speed Graph 1250m 51

Figure 3.25. Controlled Traffic Density Heatmap(seed=37 CD=750m PR=50%) 52

Figure 3.26. Controlled with Predicted Traffic Density Heatmap(seed=37 CD=750m PR=20% 53

Figure 3.27. Controlled with Predicted Traffic Density Heatmap(seed=37 CD=750m PR=50% 54

Figure 3.28. Controlled Traffic Density Heatmap(seed=37 CD=1250m PR=50%) 55

Figure 3.29. Controlled with Predicted Traffic Density Heatmap(seed=37 CD=1250m PR=20% 56

Figure 3.30. Controlled with Predicted Traffic Density Heatmap(seed=37 CD=1250m PR=50% 57

Figure 3.31. Density 3D Surface Plot for Controlled SWSCAV Method 68

Figure 3.32. Density 3D Surface Plot for Predicted SWSCAV Method 68

Figure 3.33. Controlled Traffic Density Heatmap(seed=59 CD=1250m PR=50%) 69

Figure 3.34. Predicted Traffic Density Heatmap(seed=59 CD=1250m PR=50%) 70

LIST OF TABLES

Table 3.1. Simulation parameters 13

Table 3.2. Characteristics of the vehicle types modeled in the simulation . . . 14

Table 3.3. Common scenario parameters for all tested real-time traffic management methods 16

Table 3.4. LCS Simulation Parameters 19

Table 3.5. VSL Simulation Parameters 21

Table 3.6. Convolutional Neural Network Parameters and Losses 31

Table 3.7. Example Performance Measurement Table 32

Table 3.8. Features of Each Traffic Management Method 32

Table 3.9. Percentage Change of Example Performance Measurement Table . 33

Table 3.10. Performance of SWSCAV for Each Incident Duration 36

Table 3.11. Performance of SWSCAV for Each Penetration Rate 36

Table 3.12. Performance of SWSCAV for Each Incident Lane 37

Table 3.13. Performance of SWSCAV for Each Control Distance 38

Table 3.14. Comparison of SWSCAV with Other Traffic Management Methods 43

Table 3.15. Performance of SWSCAV for Each Incident Duration 44

Table 3.16. Performance of Predicted SWSCAV for Each Penetration Rate . . 45

Table 3.17. Performance of SWSCAV for Each Incident Lane 46

Table 3.18. Performance of SWSCAV for Each Control Distance 47

Table 3.19. Comparison of Predicted Control Method with LCS and VSL . . . 58

Table 3.20. Comparison of the Predicted and Unpredicted SWSCAV by Incident Duration 60

Table 3.21. Comparison of Predicted and Unpredicted SWSCAV by Penetration Rate 61

Table 3.22. Comparison of Predicted and Unpredicted SWSCAV by Incident Lane 63

Table 3.23. Comparison of Predicted and Unpredicted SWSCAV by Control Distance 65

Table 3.24. Scenario Control Distance=1250 Penetration Rate=50 Seed=4 . . 66

Table 3.25. Scenario Control Distance=1250 Penetration Rate=70 Seed=4 . . 67

LIST OF SYMBOLS

q	Traffic Flow
k	Traffic Density
ω	Shockwave Speed
u	Speed
N	Number of Vehicles
t	Time
K	1-Dimensional Dataset
M	Multiplication factor for upsampling
S	Spacing
L	Length
G	Generator
D	Discriminator

LIST OF ACRONYMS/ABBREVIATIONS

SUMO	Simulation of Urban Mobility
LCS	Lane Control Signals
VSL	Variable Speed Limits
AV	Autonomous Vehicle
CAV	Connected Autonomous Vehicle
V2I	Vehicle-to-Infrastructure
V2V	Vehicle-to-Vehicle
V2X	Vehicle-to-Everything
SWSCAV	Shockwave Speed Connected Autonomous Vehicles
FFT	Fast Fourier Transform
Lasso	Least Absolute Shrinkage and Selection Operator
GAN	General Adversarial Networks
cGAN	Conditional General Adversarial Networks

1. INTRODUCTION

1.1. Introduction and Motivation

Congestion affects traffic mainly by increasing densities, travel times, delays, and by decreasing the safety and quality of life of passengers. Traffic incidents also reduce road capacity and cause lane closures [2]. One of the most significant reasons for congestion is incidents since incidents are unexpected events. One way to diminish the effects of incidents and improve the traffic condition is by implementing traffic management methods.

Many traffic management methods are being used in real-life traffic networks. Lane control signals (LCS), variable speed limits (VSL), ramp metering, traffic route diversion are some examples of traffic management methods. These methods mainly aim to utilize the infrastructure better to mitigate congestion and improve traffic safety.

Novelties in technology have enabled the introduction of new techniques and agents into traffic management systems. The efficiency of traditional traffic management methods is also seen to be increasing by the implementation of technological features. There are many studies in the literature regarding the utilization of currently existing technology to improve traffic management systems [3–6]. These studies mainly focus on the use of the Internet of Things (IoT) to ease the collection and processing of data to detect congestion faster and respond more efficiently. Besides these improvements, autonomous vehicles (AV) and connected autonomous vehicles (CAVs) are new emerging technologies that have drawn the focus of traffic studies. Even though it is a new technology, the use of AVs in traffic is not far from today. Advancements in communication technologies have made it possible for autonomous vehicles to use vehicle-to-infrastructure (V2I) and vehicle-to-vehicle (V2V) technologies [7]. AVs that use these communication technologies are called connected autonomous vehicles because they are connected to the infrastructure and other vehicles, which eases the transmission of data.

There are many studies about the potentials of AVs and CAVs in traffic manage-

ment [8–11]. In this study, the real-time traffic management method using connected autonomous vehicles, namely SWSCAV [1] with and without prediction is tested and compared with two real-time traffic management methods using a 3-lane study network.

1.2. Autonomous Vehicle Studies in the Literature

With the rapid increase in urban population, traffic networks started facing more traffic load, which increase the volume to capacity ratio of the traffic and increase congestion [12]. The main purpose of traffic management methods is to improve traffic flow on the existing infrastructure rather than constructing new ones. Improvements to the traditional traffic management methods are still being studied; however, alongside these studies, the potential benefits of including autonomous and connected vehicles in traffic flow are also a focal point of researchers. Even though studies indicate performance enhancements regarding the utilization of AVs and CAVs in traffic flow [13, 14], there are some concerns about this integration. Because AVs and CAVs have the potential to provide mobility for non-drivers, the traffic load is expected to increase [15–17]. However, novelties in connectivity and autonomy levels of the AVs are seen to be increasing the efficiency of self-driving cars in traffic, which can compensate for the traffic load increase in means of traffic efficiency parameters.

Equipping AVs with V2V and V2I technologies and increasing the connectivity and cooperation aspects has been seen to be increasing the improvements of AVs on traffic [18, 19]. Besides these improvements, CAVs have the feature of data transmission. A study shows that traffic conditions such as incidents and congestion can be detected more quickly through the utilization of V2I technology and data transmission [20]. Additionally, market penetration rates of CAVs carry big importance on the improvements that they provide to traffic. In studies regarding the effects of the market penetration rate of CAVs, the general outcome is that improvements in traffic efficiency, safety, environmental aspects, etc., increase with increasing market penetration rates [21–23]. In different studies, an optimum market penetration rate of CAVs is indicated [24–26]. Taking into consideration that having traffic full of CAVs is not possible soon; hence, an optimum rate is used as an option. A different study

investigates the effects of different CAV market penetration rates on different incident cases [27]. One of the incident scenarios consists of 900 seconds of incident duration and an 80% CAV market penetration rate. Results of this simulated scenario show that the total travel times of the drivers decrease by 20%. In another study, the influence of vehicle-to-everything (V2X) technology on traffic efficiency is investigated under incident cases [28]. Results of the simulations indicate a 6% decrease in travel times, 9% reduction in average stop delays, and 27% reduction in average vehicle stops. In different studies, it is also seen that CAVs provide improvements, such as increased average speed and bottleneck prevention, when traffic demands are high [29, 30]. This may show that managing the traffic by CAVs in congested regions is a feasible method.

1.3. Traffic Management using CAVs in the Literature

In the literature, many studies investigate the potential of CAVs in traffic management. One advantage of using CAVs in traffic is that they can detect congestion faster than traditional detection methods. Early congestion detection helps traffic management methods in responding quicker and managing the traffic before the congestion gets too severe. Different studies show that the severity and relief duration of congestions increase with the delay in detection [31–34]. To mitigate the severity, CAVs can be used in traffic. In a study about this matter, it is stated that vehicle-to-infrastructure (V2I) communication technology used by CAVs has the advantage of detecting incidents faster by processing the collected data [35]. There are many more studies regarding the congestion detection precision and accuracy of CAVs [36–38]. These studies present promising results in the usage of CAVs at congestion detection, which highly contributes to traffic management systems' efficiency.

Novelties in autonomous vehicle technologies enabled the utilization of these vehicles in traffic management systems. Studies show that the integration of AVs and CAVs into traffic management systems increases efficiencies of the traffic management systems [39, 40]. In a study, the implementation of the traffic management method called variable speed limits and the improvements to this method using CAVs is investigated [41]. This management system aims to reduce the speeds of drivers according

to unexpected cases such as incidents and weather conditions. Results of this study indicate that existence of CAVs improves the efficiency of VSL and CAV-enabled VSL implementation reduces traffic congestion up to 7-12%. Another traffic management method, which is also widely used, is lane control signals (LCS). LCS aims to guide drivers into changing lanes when a lane downstream is unavailable. In a study regarding the effectiveness of LCS, it is seen that this method reduces travel times and increases average speeds [42]. In a different study regarding using CAVs with the LCS traffic management method, the effects of such an integration are investigated [43]. Simulations of the scenarios are performed in an environment calibrated with real-world traffic data. Results of the simulations show that CAV-enabled LCS implementation consistently outperformed real-world LCS implementation with an average increase of 18.4%, 9.6%, and 12.8% in throughput under three scenarios. The effects of different market penetration rates should also be investigated. In a study, the dynamic route guidance traffic management method is investigated under different CAV market penetration rates in a work zone case [44]. Vehicle-to-vehicle communication technology is used by CAVs to receive work zone information early and look for possible escape routes. Results of the simulations show that under 40% market penetration rate, traffic flow becomes safer, but over 40%, the traffic safety of the drivers reduces. The results of this simulation study are only related to safety measures, so there are no findings on traffic efficiency subject. Some studies analyze the integration of CAVs and ramp metering [45,46]. Results of the studies show a promising potential due to the observed improvements in traffic efficiency.

2. THEORY

2.1. Shockwave

Shockwave refers to the boundary at which flow, speed and density states on the time-space domain are changing remarkably [47]. There are six kinds of shockwave, namely rear stationary, backward recovery, frontal stationary, forward forming, backward forming, and forward recovery.

Given that there is a noticeable change in the traffic flow parameters between two road sections A (upstream) and B (downstream) Fig. 2.1. q_A, k_A, and u_A represent the flow, density and speed characteristics of section A, and q_B, k_B, and u_B represent the flow, density and speed characteristics of section B. ω_{AB} represent the shockwave speed, which occurs in-between the sections A and B. To calculate the shockwave speed, initially, the fundamental relationship equations are constructed for each section:

$$q_A = (u_A - \omega_{AB})k_A \tag{2.1}$$

$$q_B = (u_B - \omega_{AB})k_B \tag{2.2}$$

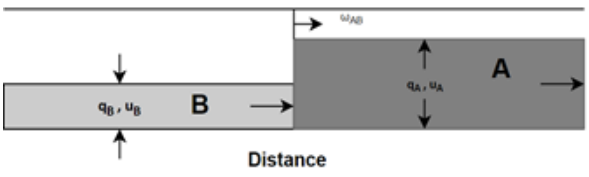

Figure 2.1. Shockwave parameters at state A and state B

N_B represents the number of vehicles, which leave B and N_A represents the number

of vehicles, which enter A. N_B and N_A are equal to each other because the number of vehicles leaving B must be equal to the number of vehicles entering A since there is no addition or removal of vehicles. Values of N_B and N_A can be found with the following equations:

$$N_A = q_A t = (u_A - \omega_{AB}) k_A t \tag{2.3}$$

$$N_B = q_B t = (u_B - \omega_{AB}) k_B t \tag{2.4}$$

Solving the equation for ω_{AB} we get:

$$\omega_{AB} = \frac{q_A - q_B}{k_A - k_B} \tag{2.5}$$

2.2. Fast Fourier Transform (FFT) Upsampling

Fast Fourier Transform (FFT) is an algorithm that is used to calculate Discrete Fourier Transforms and enables filling of data gaps by making a signal approach to spatial and temporal data. In this algorithm, the discretized equivalents of the data points to be filled are calculated by transferring the data to the frequency domain by trigonometric interpolation [48]. This sampling transformation can be applied to data of any dimension, which means that the algorithm can be applied to 1-dimensional data, image data, and any data in the time or space domain. In the process of up-sampling, first, the number of data points is equalized to the target data number with the zero-stuffing method. The purpose of this process is to do the interpolation correctly and save processing power. The zero-stuffing process is shown in Equation 2.6.:

$$K_{zero-stuffed}[\chi] = \begin{cases} K_t[\frac{\chi}{M}], & \frac{\chi}{M} \in z \\ O, & \text{else} \end{cases} \qquad \chi = 1, 2, 3, 4...., N \tag{2.6}$$

where K_t is the 1-dimensional data array for which up-sampling is intended. $K_{\text{zero-stuffed[x]}}$ is the x-th value of 1-dimensional zero-stuffed dataset $K_{\text{zero-stuffed}}$. $K_{\text{zero-stuffed}}$ is simply the dataset where zero values are inserted between each successive pair of the input data point. M is the multiplication factor, which must be an integer. N is the target number of the data points of the up-sampled data array. N is simply the product of the length of K_t and M. Spacing between two adjacent data points of $K_{\text{zero-stuffed}}$ can be calculated as below:

$$S_{zero-stuffed} = \frac{L_{K_t}}{N} S_{K_t} \tag{2.7}$$

, where $S_{\text{zero-stuffed}}$ is the space between two successive data points of the up-sampled array, $L_{K_t}$is the length of the K_t and S_{K_t} is the space between two adjacent data points of the initial array. After $K_{\text{zero-stuffed}}$ is obtained, the data is up-sampled by applying FFT transformation, assuming that the data exhibits signal behavior. Each element in the up-sampled data array is calculated with Equation 2.8. shown below:

$$K_{up-sampled}[\chi] = \sum_{n=0}^{N} K_{zero-stuffed}[n] * e^{\left(\frac{-2*\pi*i}{N}*\chi*n\right)} \qquad \chi = 0, 1, 2, 3...., N \tag{2.8}$$

where $K_{\text{upsampled}}[x]$ is the x_{th} data point of a 1-dimensional upsampled data array. Figure 2.2. is an illustration of the relationship between initial traffic density data and up-sampled traffic density data. Blue dots represent traffic density data collected by the detectors, and orange dots represent up-sampled traffic density data.

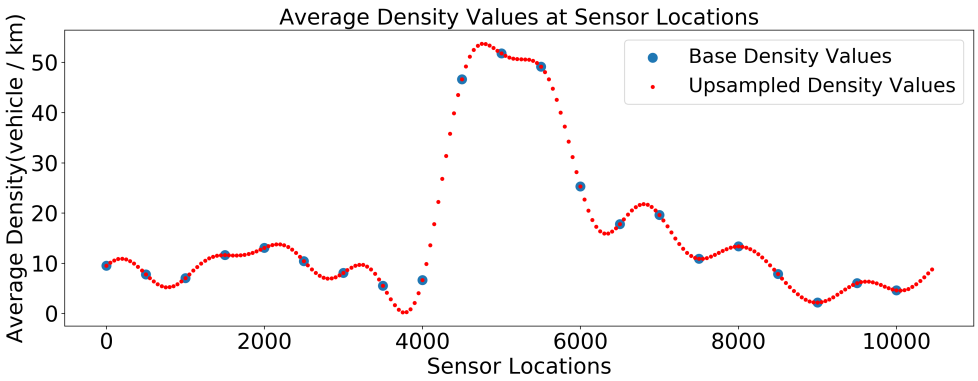

Figure 2.2. Fast Fourier Upsampling applied to the sample of traffic density data

2.3. Fused Lasso

The Lasso (Least Absolute Shrinkage and Selection Operator) is a statistical method that includes both variable selection and regularization. The Lasso regularizes the model variables by penalizing their coefficients, even reducing some of them to zero.

The Fused Lasso is a data smoothing technique used for both spatial and temporal datasets to observe significant pattern changes. $\hat{\beta}$ coefficients in the Fused Lasso method should satisfy the following Equation 2.9. and Equation 2.10.:

$$\hat{\beta} = arg\ min\left\{ \sum_{i}^{N} \left(y_i - \sum_{j} \chi_i \beta_j \right)^2 \right\} \tag{2.9}$$

subject to

$$\sum_{j=1}^{p} |\beta_j| \leq s_1 \quad \text{and} \quad \sum_{j=2}^{p} |\beta_j - \beta_{j-1}| \leq s_2 \tag{2.10}$$

where N is the total number of cases having outcomes y_1, y_2, $y_3 \ldots y_n$ and features x_{ij}, where i = 1,2,3...N and j = 1,2,3...p. The first constraint, s1, encourages sparsity in the coefficients; the second, s2, encourages sparsity in their differences, i.e. flatness of the coefficient profiles β_j as a function of j [49]. The second constraint shrinks the absolute

differences between successive data points of y, thus it provides a piecewise constant solution. In Figure 2.3., Fused Lasso is applied to a 1-dimensional sample up-sampled traffic density array. The red line is the 1-dimensional Fused Lasso approximation solution which is the smoothed traffic density distribution, and blue dots are the up-sampled traffic density data. Traffic density values close to each other are clustered in the form of a straight line.

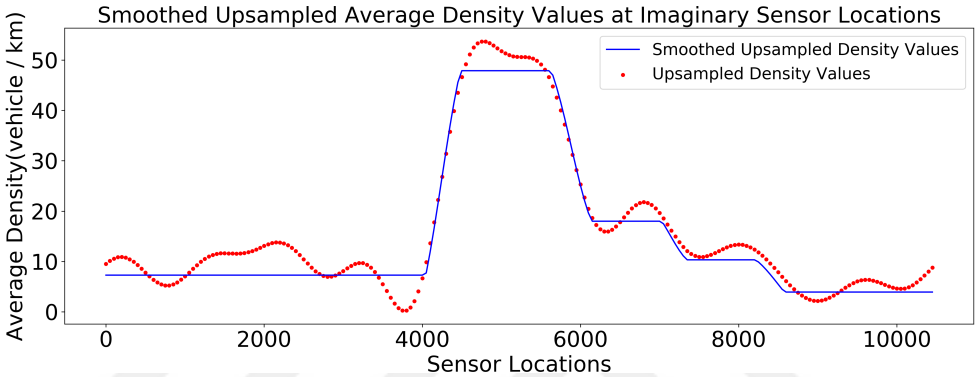

Figure 2.3. Up-sampled traffic density data with Fused Lasso application

2.4. Pix2Pix Generative Adversarial Networks Algorithm

Pix2Pix General Adversarial Networks (GAN) is a conditional GAN (cGAN) architecture designed to transform an image into a different image in the same dimensions. cGAN is a type of GANs, in which the output of the model is conditionally dependent on an input, which is the input image for Pix2Pix. Pix2Pix architecture consists of two parts. The first one is the generator model that creates the fake image from the input image, the second is the discriminator model that tests whether the synthetic image created by the generator is real or not. During the training process of the model, the generator is trained with adversarial loss according to the response from the discriminator, while the discriminator is updated via L1 loss directly. Simultaneous training of these two different models allows the generator to be better trained to "trick" the discriminator and at the same time, the discriminator can make

the discriminations more accurately. The loss function of the cGAN models is given in Equation 2.11.

$$\mathcal{L}_{cGAN}(G, D) = \mathbb{E}_{x,y}[\ \log D(x, y)\ ] + \mathbb{E}_{x,z}[\ \log\left(1 - D(x, G(x, z))\right)\ ] \tag{2.11}$$

where x is the observed image, z is the random noise vector, y is the output image, G is the trained generator model, D is the trained discriminator model. Thus, G(x,z) is simply trying to reach to y. G tries to minimize this loss function and D maximize the loss function, so that the images created by G cannot be distinguished from real images as much as possible and D can discriminate that the visuals created by G are fake. However, the generator's only task is not to "trick" D, but also to bring the output image closer to the input image. Traditional L1 distance rather than L2 distance is selected to train G in Pix2Pix algorithm to reduce unclearness as shown in Equation 2.12.

$$\mathcal{L}_{L1}(G) = \mathbb{E}_{x,y,z}[\ ||y - G(x, z)||_1\ ] \tag{2.12}$$

Thus, the final objective function of Pix2Pix is:

$$G^* = arg\ \min_G \max_D\ \mathcal{L}_{cGAN}(G, D) + \lambda \mathcal{L}_{L1}(G) \tag{2.13}$$

In Figure 2.4., The traffic density heat map estimated by Pix2Pix algorithm is shown. The left-most image is the input heatmap image, the image in the middle is the target image and the right-most image is the predicted density heatmap image.



Figure 2.4. Measured input density image(left-most), target density image(middle) and predicted density image(right-most)

3. METHODOLOGY

The flow chart of the methodology is presented in Figure 3.1.

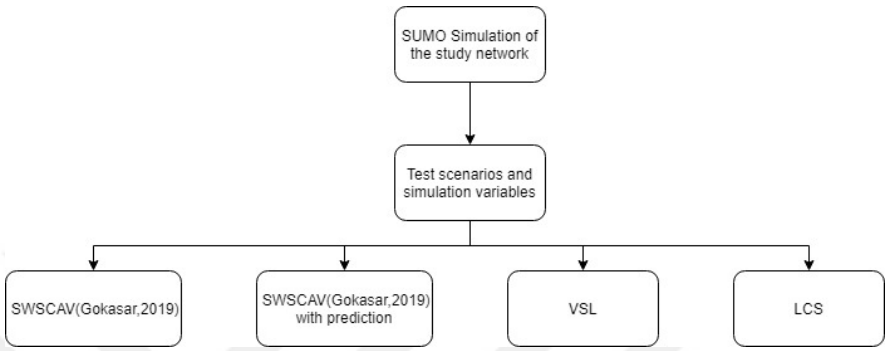

Figure 3.1. Flow chart of the methodology.

3.1. Simulation of the Study Network using SUMO

The open-source SUMO traffic simulation software is used for the evaluation of the real-time traffic management methods since it enables the agent to exploit run-time simulation with the TCP-based client-server architecture library in Python 3.6. (TraCI). In the road networks created in SUMO, road geometry and properties, sensor types and locations, vehicle types and characteristics, and traffic flow values are provided as input.

The study network is 11 kilometer-long. The first and last 250 meters of this network are modeled as sections separate from the main road section so that the speed changes of vehicles while entering to and leaving from the simulation do not affect the analysis data. The road segments modeled in the simulation are as follows:

i. Entry section (250 meters).
ii. Main section (10.500 meters).
iii. Exit section (150 meters).

The road consists of 3 lanes and the width of each lane is 320 centimeters. Sensors are placed every 500 meters. The illustration of the road network is given in Figure 3.2. Yellow lines indicate sensor locations.

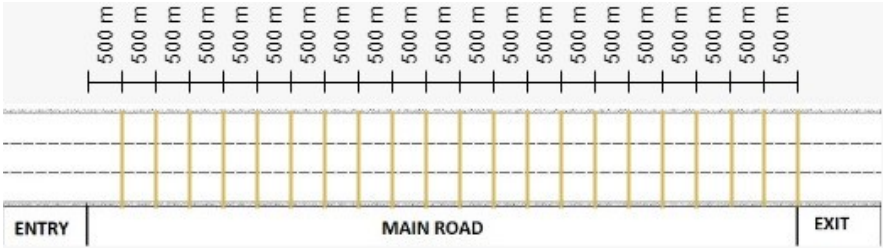

Figure 3.2. The study network

Simulation parameters are given in Table 3.1.

Table 3.1. Simulation parameters

Parameter	**Value**
Simulation period	90 Minutes
Maximum Speed (V_{max})	110 km / hr
Detector time-frequency for data collection	15 Seconds
Distance between detectors	500 meters
The total length of the road	10500 meters

The vehicle parameters are then defined in the SUMO environment. In this study, there are two different vehicle types in the road network which are vehicles with drivers and connected autonomous vehicles. Vehicles with drivers are prone to making mistakes or reacting late to traffic events and signs. The other vehicle type is connected autonomous vehicles. This vehicle type reacts in a shorter time and obeys the signs. The characteristics of the vehicle types modeled in the simulation are shown in Table 3.2.

Table 3.2. Characteristics of the vehicle types modeled in the simulation

Vehicle Parameter	**Vehicle with Driver**	**Connected Autonomous Car**
Maximum Acceleration	2.7 m/s^2	2.7 m/s^2
Maximum Deceleration	4.5 m/s^2	4.5 m/s^2
Length of vehicle	4.5 m	4.5 m
The maximum speed of a vehicle	110 km/hour	110 km/hour
Speed Factor	0.9	0.9
Minimum Gap	1.5 meters	1.5 meters
Sigma	0.4	0.05
Speed Deviation	0.35	0.1

The maximum acceleration and deceleration values are the maximum speed change values per second allowed throughout the simulation for vehicle types. During the simulation, vehicles do not move away from these values unless an otherwise command is transmitted to the vehicles via TraCI.

"Sigma" and "Speed Deviation" are two parameters that clearly distinguish these two vehicle types from each other in this study. Sigma is defined as the driver imperfection in the SUMO manual. This parameter is a Krauss car following model parameter that directly affects the awareness of the driver and regulates the variation of acceleration of the vehicles caused by a driver. It is scaled between 0 and 1, where 0 means the driver is perfect. That means the driver is fully aware and accelerates in the theoretically most smooth way. The "Speed Deviations" parameter is the standard deviation of the standardized speed distribution of that type of vehicle. CAVs demonstrate a more homogeneous speed distribution compared to vehicles with drivers, the speed values of CAVs should be grouped more around the center value.

3.1.1. Assumptions of the Network

i. In the simulation, there are autonomous vehicles and vehicles with drivers. Both vehicles are 4.5 meters long.
ii. Krauss vehicle tracking theory is the default vehicle tracking theory used in this study.
iii. The two variables that distinguish autonomous vehicles from driven vehicles are driver imperfection (sigma) and speed deviation.
iv. Connected autonomous vehicles follow the given instructions without any exception.
v. It takes one second for connected autonomous vehicles to receive information from the sensors and take action.
vi. It is assumed that the connected autonomous vehicles know their location clearly at any time.
vii. It is assumed that the connected autonomous vehicles in traffic converge linearly to the shock wave speed with a pre-determined acceleration/deceleration.

3.1.2. Simulation Workflow

In this thesis, each simulation scenario was run in a statistically sufficient number of 6 different ways in total. These are: there are no CAVs, CAVs are available but traffic is not managed, and traffic is managed by four different traffic management method (SWSCAV [1] with and without prediction, LCS, and VSL).

3.1.3. Common Scenario Parameters

These variables are the percentage ratio of the number of CAVs in traffic to the number of all vehicles, the occurrence time, the duration and the position of the incident, the lane where the incident occurred, and the length of the accident duration. The simulations were run by selecting a completely random integer value for each seed from the ranges of these variables, given in Table 3.3. The ratio of connected vehicles

is equal to the ratio of the number of connected vehicles to the number of all vehicles in traffic. Since the traffic flow value in this study was determined as 1500 vehicles per hour per lane, the 10% CAV ratio corresponds to 150 CAV per hour per lane. The incident time is randomly decided through the occurrence time of the incident, in seconds, of the simulation at the beginning of the simulation. The incident duration and incident position are predetermined values at the beginning of the simulation. The incident time controls how long the accident will last and the incident position is where the accident occurs. The random lane value controls in which lane of the road the incident will occur. Besides these variables, each traffic management method has its variables.

Table 3.3. Common scenario parameters for all tested real-time traffic management methods

Parameter	**Range**
Connected Vehicle Ratio (%)	[10,20,30,40,50,60,70,80]
Incident Time(sec)	Random integer in the range of (900,2700)
Incident Duration(sec)	Random integer in the range of (600,1500)
Random Position(meter)	Random integer in the range of (4500,8000)
Random Lane	[0,1,2]*

*where 0 = Right lane , 1 = Middle lane and 2 = Left Lane

3.1.4. Data Collection and Storage Process

In this study, average flow, density, and velocity values are used for analysis. For this reason, only these data were collected from the sensors to use both processor power and storage capacity efficiently. In each lane of the road network, a sensor is placed every 500 meters. (Figure 3.2). That is, there are 3 different sensors in the road network, one in each lane for every 500 meters which means there are 21 sensor locations in a 10,500 meter-network. These sensors collect data every 15 seconds. The flow, density, and speed values read from these three sensors are averaged to obtain

the general state of the road depending on time and location using Equation 3.1:

$$\chi_{i,t} = \frac{\chi_{i_0,t} + \chi_{i_1,t} + \chi_{i_2,t}}{3} \qquad i = 1, 2, 3..., 21 \tag{3.1}$$

,where x can be one of the flow, density, or speed values collected from a sensor, i is the indicator of sensor location.x_{i_0},x_{i_1} and x_{i_2} indicates the value read on the ith sensor in the right, middle and left lanes respectively. In later stages, for data from sensors, instead of x, the notations q for flow, k for density, and v for speed will be used.

Flow values are stored by converting the total number of vehicles recorded in the sensors for 15 seconds to the number of passing vehicles per hour. This transformation is given in Equation 3.2:

$$Q_{i,t} = \frac{q_{i,t} \times 3600}{15} \qquad i = 1, 2, 3..., 21 \tag{3.2}$$

,where, Q_i is the transformed flow value to store.

Speed values are calculated by storing and averaging the speeds of each vehicle passing through the sensor location. This calculation is given in Equation 3.3:

$$V_{i,t} = \frac{\sum_{k=0}^{k=N} v_{(i,t),k}}{N} \qquad i = 1, 2, 3..., 21 \tag{3.3}$$

,where; $V_{i,t}$ is the speed value at position i stored to be analyzed, $v_{(i,t),k}$ is the speed of the kth vehicle measured instantaneously at that location and N is the total number of vehicles detected by the ith sensor at any time.

Density values cannot be obtained directly from the simulation. Occupancy values measured from the sensors are converted into density. The formula used in the transformation is given in Equation 3.4

$$K_{i,t} = \frac{o_{i,t}}{L + d} \qquad i = 1, 2, 3..., 21 \tag{3.4}$$

where, K_i is the density value at position i stored to be analyzed, o_i is the occupancy value read by i_{th} sensor, L is the length of a vehicle and d is the length of the detector.

3.1.5. LCS Implementation

Lane control systems (LCS) is a real-time traffic management method applied for a more stable and safe operation of lanes in freeways. This goal is achieved by electronic signs placed above the lanes informing drivers to change their speed or lane. LCS screens on a 4-lane road are shown in Figure 3.3.

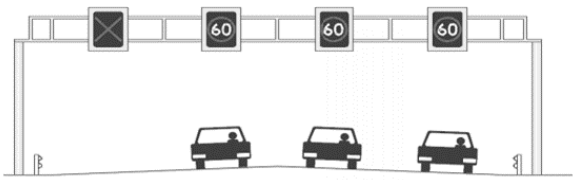

Figure 3.3. Illustration of LCS Implementation on a 4-Lanes Road (TRUMM, 2010)

In this study, the following assumptions were made while implementing LCS:

i. Lane control signs start 300 seconds after an incident occurs. Also, these signs continue to run for up to 300 seconds after the incident completely is removed.
ii. Drivers notice these LCS signs 30 meters before the first sign away further away from the incident and take action within a maximum of 2 seconds
iii. While connected autonomous vehicles obey LCS without exception, regular vehicles follow LCS with some compliance rate.
iv. Two LCS are placed in the system. The first one is placed in the first sensor position just before the accident (LCS 1), the second is placed a control distance away from the LCS 1 (LCS 2). Sensor locations during an incident are given in Figure 3.4. In Figure 3.4, the yellow lines show the sensor positions and the pink rectangle provides the incident position.
v. If the LCS shows the lane change sign:
    a. In the right lane: Lane change is towards the middle lane.
    b. In the left lane: Lane change is towards the middle lane.
    c. In the middle lane: The lane is towards a randomly selected one from the

right or left lane.

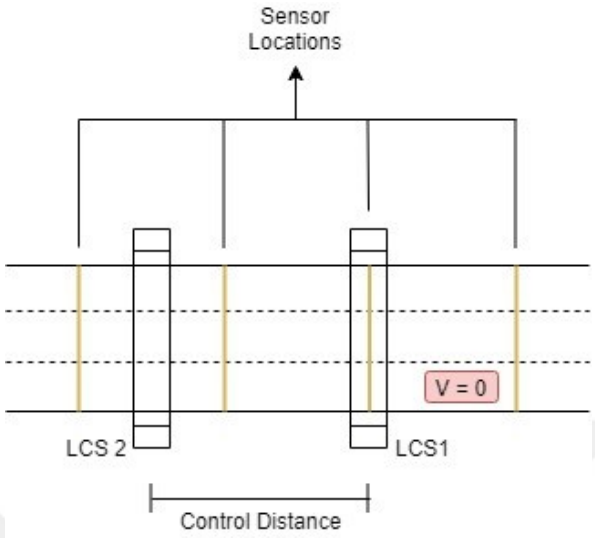

Figure 3.4. Sensors Locations

Drivers' responses to LCS 1 and LCS 2 differ from each other in terms of compliance rate [50]. Using a trial-and-error method through an extensive number of simulations, the optimum parameters for LCS implementations are selected [1]. The simulation parameter values of the LCS implementation are given in Table 3.4.

Table 3.4. LCS Simulation Parameters

Parameter	**Value**
LCS 1 Compliance Rate (%)	80
LCS 2 Compliance Rate (%)	70
Control Distance (meter)	1000

The LCS compliance rate gives the probability that a vehicle within the range of the LCS 1 will comply with its signs. It should be recalled that CAV vehicles obey these signs completely. The control distance represents the distance between LCS 1 and LCS 2. The flow chart of the LCS implementation is given in Figure 3.5.

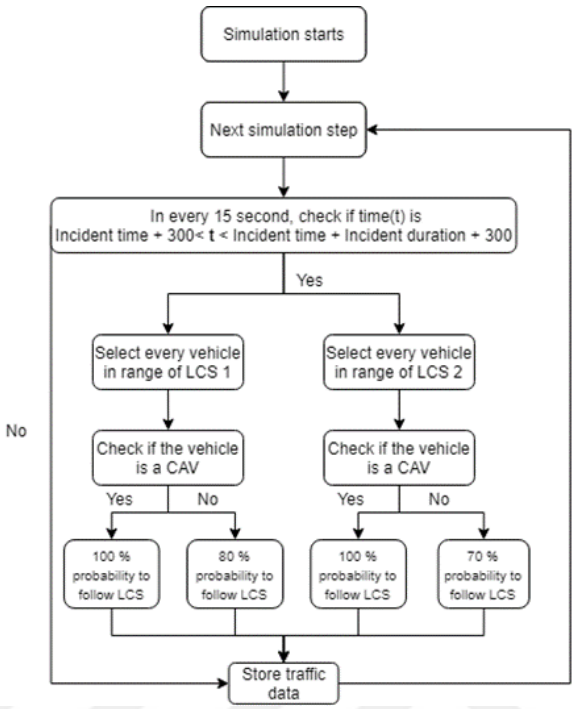

Figure 3.5. The flowchart of LCS implementation

3.1.6. VSL Implementation

The Variable Speed Limit (VSL) is a real-time traffic management method. It is based on the principle of managing the traffic by regulating the speed of the vehicles in conditions such as traffic congestion. In this study, the following assumptions were made while implementing the VSL:

i. VSL signals start to inform drivers 300 seconds after an incident occurs. Also, these signals continue to run for up to 300 seconds after the incident completely is removed.
ii. Drivers notice these signals 30 meters before the first signal upstream and take action within a maximum of 2 seconds.
iii. Drivers following the signs reduce their speed to the recommended speed as early as possible.

iv. While connected autonomous vehicles comply with the VSL signals without exception, vehicles with drivers follow these signs with a certain compliance rate.

v. v. There is only one VSL signal. This signal is placed as far back as the control distance from the accident location. The visual representation of the VSL signal location is given in Figure 3.6.

vi. VSL signs in each lane show the same target speed.

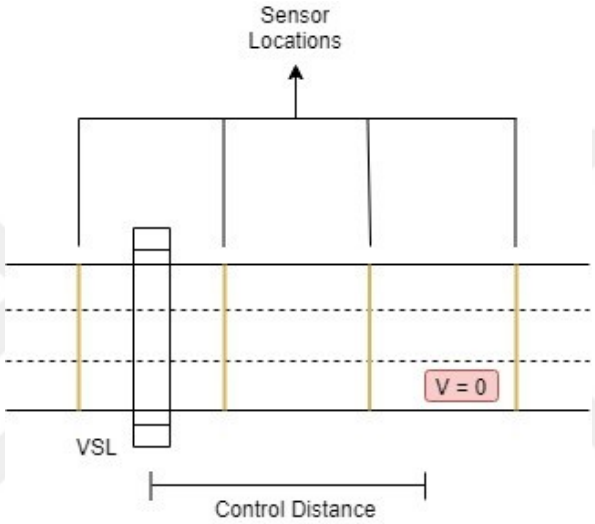

Figure 3.6. The sketch of the study network for VSL implementation

VSL parameters giving the best results are presented in Table 2.5 obtained through a comprehensive simulation study [1].

Table 3.5. VSL Simulation Parameters

Parameter	**Value**
Compliance Rate (%)	50
Control Distance (meter)	1000
Target Speed (km/hour)	40

The compliance rate shows at what rate the vehicles with driver obeys the VSL signal. The target speed indicates the speed value at which the vehicles need to be adjusted their speeds. The control distance shows how far behind the vehicles will start to be managed from the accident location. VSL implementation flowchart is given in Figure 3.7.

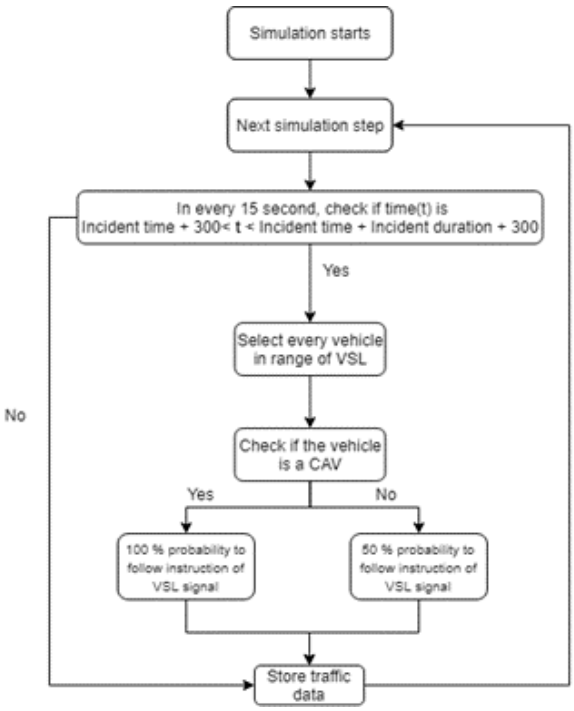

Figure 3.7. VSL simulation flowchart

3.1.7. SWSCAV [1] Implementation

This implementation uses multiple mechanisms simultaneously to provide dynamic management of traffic.

SWSCAV [1] is based on managing the speeds of the connected autonomous vehicles in traffic during the presence of any shockwave, starting from the control distance of the boundary opposite to the direction of the traffic flow. In this study, the following assumptions were made while modeling SWSCAV [1]:

i. Connected autonomous vehicles constantly know their location very accurately and can receive information from infrastructure.
ii. Connected autonomous vehicles implement the given directive as soon as possible without any exception.
iii. Connected autonomous vehicles reduce their speed linearly to equal their speeds to shockwave speed when it reaches the upstream direction of the shockwave.
iv. Momentary traffic density data based on the location shows wave behavior.
v. Vehicles cannot exceed the maximum speed of the road and do not apply when a speed lower than 10 km / h is recommended.

In this process, sensor data collected every 15 seconds is used to check whether a shock wave is present at that time. After the shock wave is detected, the sensor data is up-sampled to prevent underutilization caused by the distance between the sensors. The up-sampled data is smoothed to remove noise and sensor error. Then, using this up-sampled and smoothed density and flow data, the position of the boundary of the shockwave located upstream of the traffic and the speed of the backward shockwave is calculated. This calculated speed is then transmitted to the connected autonomous vehicles that are as far back as the control distance from the shock wave boundary in traffic, and the connected autonomous vehicles regularly adjust their speed to the shock wave speed. The flow chart of the SWSCAV [1] is given in Figure 3.8.

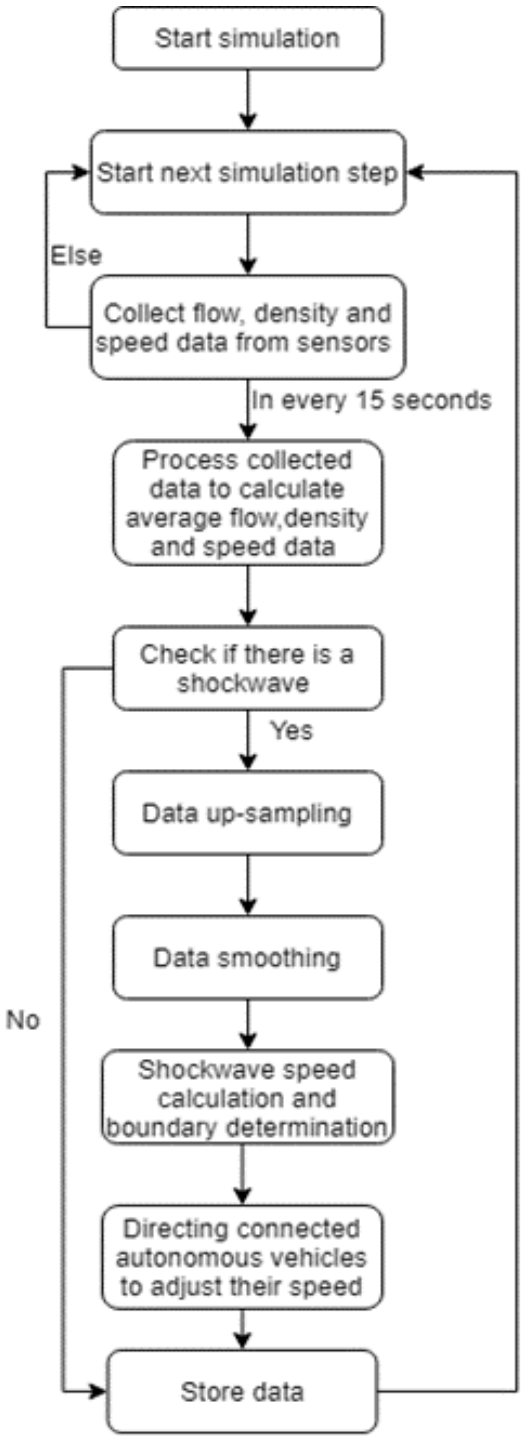

Figure 3.8. Flowchart of SWSCAV [1] Implementation

3.1.7.1. Shockwave Detection. During simulations, every 15 seconds, the flow, occupancy, and speed values collected from sensors are placed on every 500 meters. These

data are processed to calculate average flow, density, and speed values at sensor locations. These data are used to detect the shockwave and after advanced processing, to find the shockwave boundary of the traffic upstream. The pseudo-code of shock wave detection is given in Figure 3.9. Critical density was determined as 38 vehicles per kilometer by preliminary work. This value is the lowest traffic density value where congestion is observed in a region. According to Figure 3.9, if the average density at a location is greater than 38 veh / km for 15 seconds and the average speed in that area falls below 30 km / h, that location indicates the presence of a shock wave.

```
# We do not observe any shockwave before incident time. So, we save process power.
if (step > incident time):
   # We do not expect first 800 meters to be congested
   for x in sensor locations:
      if ((average density at x > critical density) & (average density at x 15 second before > critical density)):
         if (calculated speed at x < 30):
            detectionstatus = True
            break
         else:
            detectionstatus = False
      else:
         detectionstatus = False
```

Figure 3.9. Shockwave Detection Algorithm

3.1.7.2. Application of Data Up-sampling. After the shock wave has been detected, further procedures should be performed to determine the speed and location of the shock wave more accurately. In the road network used in this study, sensors were placed on the road at 500 meters intervals. While the 500-meter sensor range may be sufficient to provide information on the current state of traffic, the situation where sensors are placed more frequently than 500-meter intervals can be converged to fine-tune with data

processing techniques. In this study, the Fast Fourier Transform (FFT) Upsampling method is used to make the sensor arrangement placed every 500 meters approach the question of the sensor placed every 50 meters. In this study, it is assumed that the instantaneous density values of traffic show wave behavior during the simulation. The basic principles of the FFT process are given under the theory section. Traffic density and flow data are up-sampled to determine the speed and location of the shockwave. There is no need to up-sample speed data. In Figure 3.10, traffic density values are provided according to the sensor positions during a shockwave. Figure 3.11 shows the up-sampled traffic density data. When the two shapes are examined, the wave behavior approach can be seen clearly. For the remainder of this study, each of the red dots in Figure 3.11 will be treated as if there were sensors.

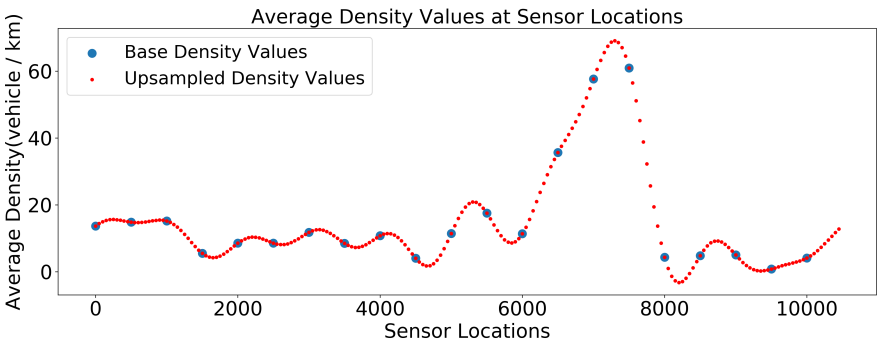

Figure 3.10. Average Density Values at Sensor Locations

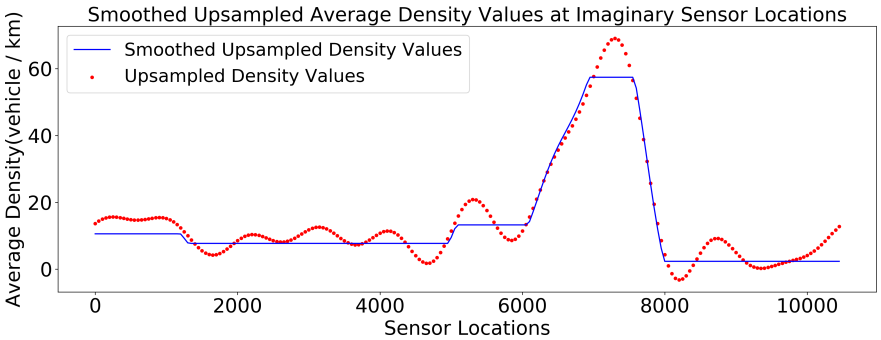

Figure 3.11. Up-sampled Average Density Values at Sensor Locations

3.1.7.3. Application of Data Smoothing. After the data was sampled up, the Fused Lasso algorithm was used to minimize the instantaneous measured error, minimize the effect of outlier values while processing the data, and determine the important change points in the data. The basic principles of this algorithm are given in the 'Theory' section under the title of 'The Fused Lasso'. In this study, the Fused Lasso algorithm is used to determine the boundaries of the shock wave and to calculate the shock wave velocity. In Figure 3.12, the up-sampled data shown in Figure 3.11 is processed with the Fused Lasso algorithm. The data point having the lowest average density value above the critical density value at the left-hand side of the peak formed on the data is the upstreaming boundary point of the shock wave of the traffic. The upstreaming shock wave boundary is shown in Figure 3.12 as a purple dot.

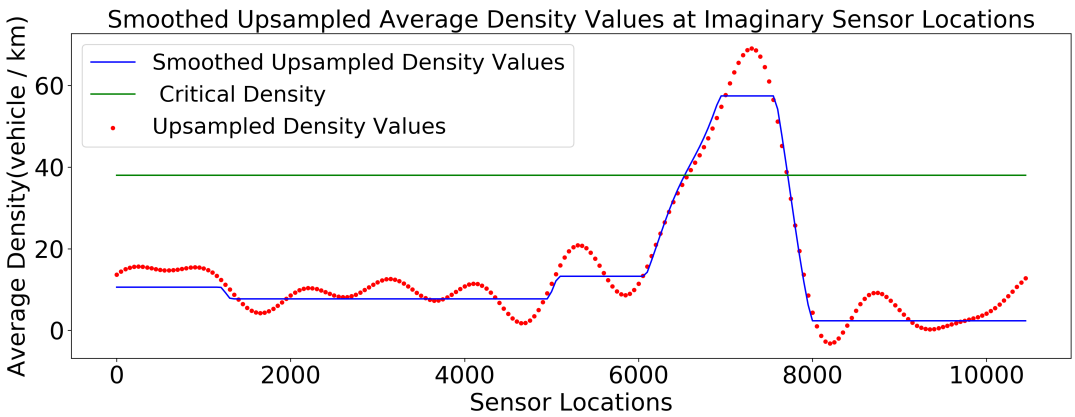

Figure 3.12. Smoothed Up-sampled Average Density Values at Sensor Locations

3.1.7.4. Shockwave Speed Calculation. Until this stage, the data collected from the sensors were processed and the positions of the imaginary sensors and the average flow and density values were obtained. In Figure 3.12, the sensor location, which is the shockwave boundary, is given as a pink dot. That location is referenced to calculate the shockwave speed. The shockwave speed calculation is given in Equation 3.5.

$$v_{sw} = \frac{q_x - q_{x-1}}{k_x - k_{x-1}} \tag{3.5}$$

,where v_{sw} is the shockwave speed, q_x and k_x are the average flow and density values, respectively at the shockwave boundary sensor, and q_{x-1} and k_{x-1} are the average flow and density values, respectively, at the sensor just behind the shockwave boundary sensor. And finally, this calculated shockwave speed is transmitted to connected autonomous vehicles within control distance to adjust their speed to that speed.

3.1.8. SWSCAV with Prediction [1] Implementation

The difference between the SWSCAV with Prediction [1] and SWSCAV [1] is that the main data used to determine the shockwave location and velocity are taken from a row of an estimated heat map, not from the instantly collected data. Also, a row of predicted 2-minutes estimated heatmap of 2 minutes later is used for data processing. The flow chart describing the implementation of SWSCAV with Prediction [1] in the simulation environment is shown in Figure 3.13.

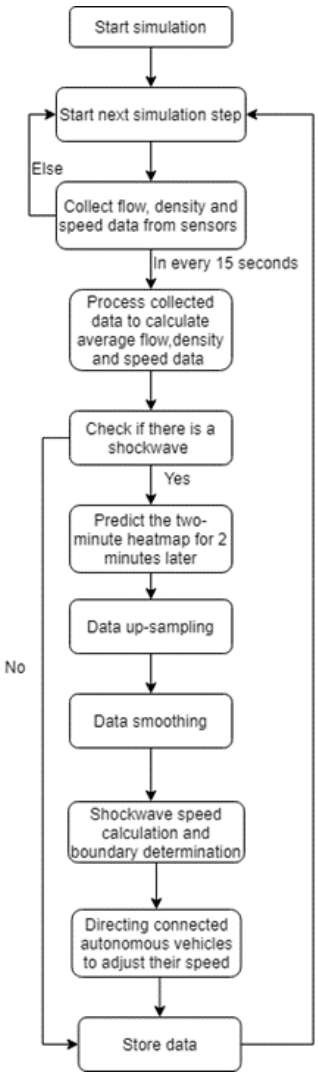

Figure 3.13. The flow chart of the implementation of SWSCAV with the prediction [1]

The data used for processing are density and flow data exactly 3 minutes after the instantaneous time. For example, suppose a shockwave is detected at the 30th minute of the simulation. Using the stored flow and density data between the 28th and 30th minutes of the simulation, flow and density heat maps between the 32nd and 34th minutes of the simulation are estimated. As the data is collected every 15 seconds, the size of the 2-minute heat maps consists of 21 columns (sensor locations) and 8 lines (15 seconds timesteps). Pix2Pix deep learning algorithm was used in this prediction process. The basic principles of this learning algorithm are given in the "Theory"

section.

3.1.8.1. Training and Implementation of Pix2Pix Algorithm. For heatmap predictions, Pix2Pix image-to-image algorithm is selected. For this algorithm to work, one image input with the same size as the desired output image must be given. In this study, it was decided to estimate the two-minute heatmaps. Therefore, two-minute heatmaps should be given as input. To train the prediction model to be used in this study, heatmaps sections were taken from the base scenarios where only the incident occurred but not managed. Since the prediction model will only be used in the presence of a shockwave, no heat map has been obtained except in cases of the shockwave. In this way, the prediction model is enabled to make more accurate predictions in the presence of a shockwave. 13125 input images and 13125 output images, which were collected from scenarios in which only the accident occurred but was not managed, were used in the training process of the model. To ensure that the model is trained with the lowest loss, several different Convolutional Neural Network hyperparameters have been used and the model has been trained with the hyperparameters that give the lowest loss. Model parameters and losses are given in Table 3.6. In this table,

- The “Neural Network Architecture” column shows how many neurons are in each layer in the neural network architecture consisting of 7 layers.
- The ”Convolution Filter Size” column shows the size of the window that strides over the image during the training of the model.
- The ”Dropout” column shows the rate of dropout used to prevent the model from overfitting, to increase its performance, or to save CPU/GPU power.
- The “Discriminator Real Loss” column is a measure of the discriminator’s success in detecting the real image.
- The “Discriminator Generator Loss” column is a measure of the discriminator’s success in detecting the generating image.
- The “Generator Loss” column shows how successful the generator is in deceiving the discriminator.

Table 3.6. Convolutional Neural Network Parameters and Losses

Architecture Number	**Neural Network Architecture**	**Convolution Filter Size**	**Dropout**	**Discriminator Real Loss**	**Discriminator Generator Loss**	**Generator Loss**
1	8-16-32-64-64-1	2x2	0.5	0.544	0.377	5.579
2	16-32-64-128-128-1	2x2	0.5	0.195	0.409	4.527
3	32-64-128-256-256-1	2x2	0.5	0.274	0.376	2.689
4	32-64-128-256-256-1	2x2	False	0.345	0.357	1.571
5	32-64-128-256-256-1	2x2	0.2	0.327	0.355	1.671
6	32-64-128-256-256-1	3x3	False	0.345	0.351	1.691
7	32-64-128-256-256-1	4x4	False	0.351	0.359	1.641

According to Table 3.6, Architecture 4 has been selected because it gives the lowest values for "Generator Loss" and the other loss values are also low. After the model was trained, the trained model was used for real-time prediction in simulation. Flow and density data recorded every 15 seconds throughout the simulation are stored for 2 minutes. If a shock wave is detected, flow and density data stored for the last two minutes are inserted as input to the model. The output obtained is the 2-minute flow and density heatmaps of the 2 minutes later. The row in the middle of the estimated heatmap, that is, 3 minutes after the instantaneous situation, starts to be subjected to the data processing process starting from section 3.1.7.2. to 3.1.7.4.. In other words, traffic is managed according to the situation 3 minutes after the instant, not the instant situation.

3.1.9. Measures of Effectiveness

To assess the improvements related to the real-time traffic management methods, various performance criteria parameters are determined. Selected performance criteria

are specified in Table 3.7.

Table 3.7. Example Performance Measurement Table

Features	**Base**	**Uncontrolled**	**LCS**	**VSL**	**Controlled**	**Predicted**
K > 38(%)	3.81	3.48	3.52	3.28	3.12	2.27
K > 28(%)	4.24	3.72	4.18	3.68	3.76	3.01
Overall Avg. K	12.19	10.93	11.24	10.89	10.97	10.72
Overall Avg. Speeds (km/hour)	64.68	72.47	71.14	72.43	71.84	71.94
Shockwave duration (min)	27.25	27.25	27.25	27.25	27.25	27.25
Shockwave length (meter)	3000	3000	3000	3000	3000	3000
In CR K > 38 (%)	35.71	32.99	33.51	31.17	29.61	21.43
In CR K > 28 (%)	39.48	34.81	38.96	34.68	35.45	28.44
In CR Avg. Speeds(km/hour) (%)	38.59	44.19	40.77	44.54	41.19	39.92

Compared scenarios in Table 3.7 consist of base scenarios and uncontrolled, LCS, VSL, controlled (SWSCAV: Gokasar, 2019), and predicted methods (SWSCAV with the prediction: Gokasar, 2019). These scenarios differ according to the variables present in the first column of Table 3.8.

Table 3.8. Features of Each Traffic Management Method

	Base	**Uncontrolled**	**LCS**	**VSL**	**Controlled**	**Predicted**
Incident	Present	Present	Present	Present	Present	Present
CAV	-	Present	Present	Present	Present	Present
Traffic Management	-	-	Present	Present	Present	Present
SWSCAV	-	-	-	-	Present	Present
Shockwave Prediction	-	-	-	-	-	Present

In Table 3.9, the data given in Table 3.7 are calculated in percent changes according to the base scenarios to be able to observe the changes more accurately. Calculations

of the percent changes are done according to the following equation

$$\%Change = \frac{V_{method} - V_{base}}{V_{base}} \tag{3.6}$$

,where

1. %Change is the percent difference between the base scenario values and the specified method's performance criteria values.
2. V_{method} is the value of the specified method's performance criteria.
3. $V_{Uncontrolled}$ is the value of the specified method's performance criteria.

Table 3.9. Percentage Change of Example Performance Measurement Table

Features	**Base**	**Uncontrolled**	**LCS**	**VSL**	**Controlled**	**Predicted**
K > 38(%)	3.81	-8.70	-7.53	-13.73	-18.04	-40.33
K > 28(%)	4.24	-12.13	-1.43	-13.10	-11.16	-28.93
Overall Avg. K	12.19	-10.37	-7.76	-10.70	-10.01	-12.08
Overall Avg. Speeds (km/hour)	64.68	12.04	9.97	11.97	11.07	11.21
Shockwave duration (min)	27.25	27.25	27.25	27.25	27.25	27.25
Shockwave length (meter)	3000	3000	3000	3000	3000	3000
In CR K > 38 (%)	35.71	-7.64	-6.18	-12.73	-17.09	-40.00
In CR K > 28 (%)	39.48	-11.84	-1.32	-12.17	-10.20	-27.96
In CR Avg. Speeds(km/hour) (%)	38.59	14.53	5.67	15.43	6.74	3.46

The initial performance measure of the simulation study is the density threshold, which accounts for the entire simulation. Density thresholds are determined as 28 and 38. These two threshold values are the breaking points of the heatmaps. Rows 'K>38' and 'K>28' represent the percent values at which density is bigger than the specified threshold values. The second performance criterion is the 'Overall Avg. K', and this measure stands for the average density of the whole simulation. The third performance criterion is the 'Overall Avg. Speeds', which is the average speed of the overall simulation. 'shockwave duration' represents the duration of the shockwave created by the

incident. 'shockwave length' corresponds to the length at which the traffic flow is affected by the incident. Because incidents create shockwaves upstream of the incident location, examining the changes corresponding to the shockwave area rather than the whole simulation is more important. Therefore, the region bounded by the 'shockwave duration' and 'shockwave length' is marked on the heatmaps to be able to observe the density changes regarding the shockwave area since the aim of this study is to improve shockwaves. In each scenario, a critical region is specified on the heatmaps just like it can be seen in Figure 3.14. After creating the critical regions, the last three performance measures are investigated, which are 'In CR K>38', 'In CR K>28', and 'In CR Avg. Speeds' since these are the values that are related to the critical region. While comparing the performance measure values of different methods, percent changes between the critical region values are considered more important.

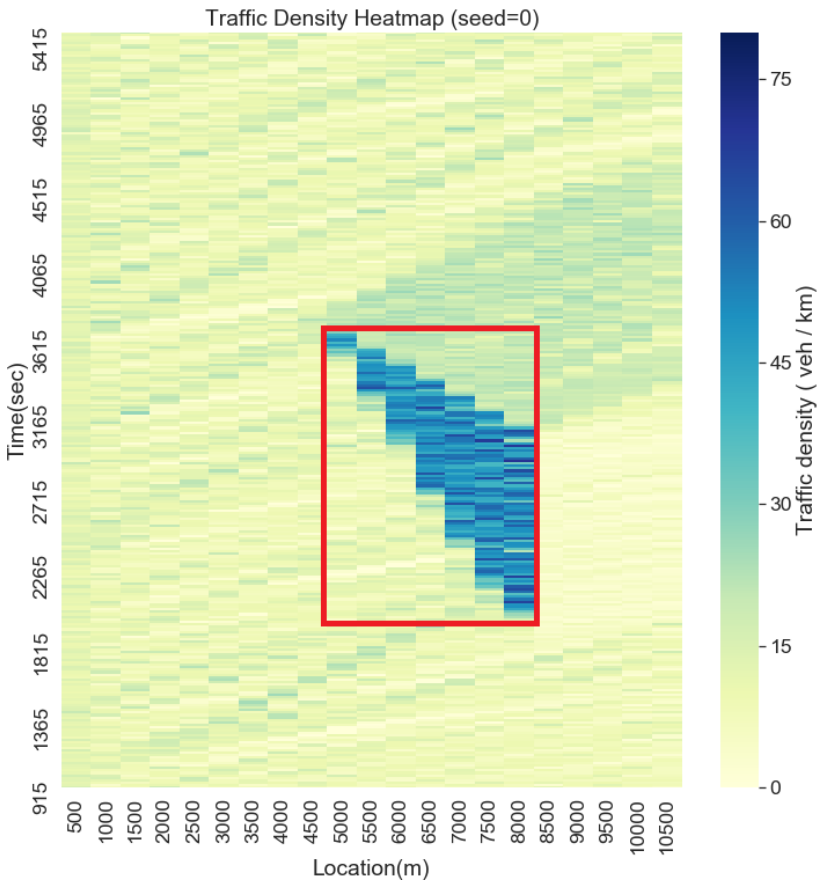

Figure 3.14. Illustration of Critical Region

Percent density values shown in Table 3.7 are calculated by dividing the area at which the density values are bigger than the specified threshold values to the entire area, making these percent values refer to the overall traffic flow. However, since the critical region is bounded by the shockwave duration and shockwave length, density values higher than the threshold values are mostly observed in the critical region. This increases the percent density values in the critical region as can be seen from Table 3.7.

Tables 3.7 and 3.9 are the results of a scenario chosen at random between 2400 different scenarios. In Table 3.9, it is observed that the controlled method reduces densities larger than 38 and 28 by 18.04% and 11.16% respectively compared with the base scenarios. It is also seen that the overall density of the traffic reduces by 10.01%. Considering these results, it is seen that the most effective improvement is observed on densities larger than the threshold of 38. This is related to the fact that; the controlled method aims to improve incident-induced shockwaves, which create high-density congestions. Therefore, the controlled method improves these highly dense areas by spreading the density to a greater area.

Improvements related to the critical region are more important since the controlled method aims to mitigate the effects of the shockwaves, which are mainly present in the critical region. In Table 3.9, it is observed that critical region densities higher than 38 and 28 is reduced by 17.09% and 10.20% respectively. Density reductions in the critical region are smaller compared to the overall simulation density reductions. On the other hand, it is seen that overall speed in the critical region is increased by 6.74%, whereas the overall network average speeds increased by 11.07%. An increase in speeds and a decrease in the percent densities indicate that the traffic flow becomes more stable with fewer speed differences. Other scenarios of the study show close trends to the results of this scenario.

The analysis provided in the following parts is all performed based on the critical region and the density threshold of 38. In Table 3.10, improvements, in short, medium, and long incident durations are shown for different CAV penetration rates based on mean and standard deviation values. The relationship between mean and standard deviation values is an important aspect of the analysis. If the decrease in

standard deviation value is higher than the increase in mean value, it means that the critical region is being stabilized. Analyzing Table 3.10, it is observed that for short and medium incident duration cases, 40% and higher CAV penetration rates show the most improvements, and for the long incident duration cases, results indicate that 50% and higher CAV penetration rates show the most improvements. It is also seen that the stability of the improvements is lower when the CAV penetration rates are low. In Table 3.11, the comparison of mean and standard deviation values with the CAV penetration rates is displayed. The difference between Table 3.10 and 3.11 is that Table 3.11 does not include the duration parameter of the incidents, so only the CAV penetration rates are discussed. Results within Table 3.11 indicate that the system works most efficiently under the penetration rates of 70% and 80%.

Table 3.10. Performance of SWSCAV for Each Incident Duration

Scenario	**CAV**	**10-15 K>38 Mean**	**10-15 K>38 Std Dev**	**Short Duration # of Scenarios**	**15-20 K>38 Mean**	**15-20 K>38 Std Dev**	**Moderate Duration # of Scenarios**	**20-25 K>38 Mean**	**20-25 K>38 Std Dev**	**Long Duration # of Scenarios**
0	10%	-32,31	39,85	85,00	-24,31	29,81	65,00	-3,08	46,97	90,00
1	20%	-39,80	32,18	85,00	-34,29	33,68	65,00	-24,67	31,92	90,00
2	30%	-43,81	30,53	85,00	-28,61	26,63	65,00	-30,37	35,14	90,00
3	40%	-51,70	28,82	85,00	-45,90	23,13	65,00	-27,71	35,81	90,00
4	50%	-54,74	25,19	85,00	-47,31	21,17	65,00	-42,21	41,62	90,00
5	60%	-52,55	27,83	85,00	-49,42	24,03	65,00	-49,79	28,54	90,00
6	70%	-55,73	29,05	85,00	-53,83	30,76	65,00	-42,63	29,22	90,00
7	80%	-54,06	24,49	85,00	-52,99	17,03	65,00	-37,76	23,62	90,00

Table 3.11. Performance of SWSCAV for Each Penetration Rate

Scenario	**Features**	**10%**	**20%**	**30%**	**40%**	**50%**	**60%**	**70%**	**80%**
0	K>38 Mean	2,04	-4,45	-1,93	-9,00	-5,97	-14,77	-16,31	-16,14
1	K>38 Std Dev	32,81	22,64	20,59	26,80	32,48	12,02	20,79	14,80
2	K>28 Mean	2,19	-2,62	2,31	-9,59	-8,23	-16,15	-2,95	-18,61
3	K>28 Std Dev	33,81	17,35	23,94	19,55	29,08	10,30	26,02	15,67
4	Scenario Number	161,00	109,00	93,00	79,00	48,00	51,00	61,00	49,00

The incident lane is the next important variable of the study because the lane at which the incident occurs distinctively affects the properties of the congestion and shockwave. For example, if the incident is located at the middle lane, lane changes affect both right and left lanes directly and interrupt the flow of both lanes, whereas it is not the same case for incidents located at right and left lanes. Table 3.12 shows the mean and standard deviation values for each lane under different CAV penetration rates. There are 105, 95, and 100 cases of incident scenarios for right, middle, and left lanes respectively, however, the formation of the shockwave is not the case for each scenario. As can be seen in Table 3.12, only 60 right lane incident scenarios, 95 middle lane incident scenarios, and 85 left lane incident scenarios contain shockwaves. Given standard deviation and mean values are calculated for the cases that contain shockwaves. Considering the ratio of the number of shockwave scenarios to the number of total scenarios for each lane, it is seen that right lane scenarios require less interference compared to other lanes. High rates of change in right lane incident scenarios can be clarified by this. Since mitigating the effects of a low severity congestion is easier, higher percentage changes are observed for right lane incident scenarios. Middle and left lane incident scenarios contain more shockwaves that are controlled by CAVs. In Table 3.13, it is seen that, as the CAV penetration rate increases, congestions decrease. It is also seen that, at a 30% CAV rate, both left and middle lane show high improvements, which is not expected.

Table 3.12. Performance of SWSCAV for Each Incident Lane

Scenario	**CAV**	**Right K>38 Mean**	**Right K>38 Std Dev**	**Right # of Shockwave Scenarios**	**Middle K>38 Mean**	**Middle K>38 Std Dev**	**Middle # of Shockwave Scenario**	**Left K>38 Mean**	**Left K>38 Std Dev**	**Left # of Shockwave Scenario**
0	10%	-12,98	60,85	60,00	-14,03	18,82	95,00	-29,31	43,77	85,00
1	20%	-45,74	38,29	60,00	-24,32	20,90	95,00	-32,67	37,18	85,00
2	30%	-44,42	30,36	60,00	-32,08	26,09	95,00	-30,64	37,58	85,00
3	40%	-46,57	48,68	60,00	-32,74	17,47	95,00	-46,68	27,98	85,00
4	50%	-65,20	46,50	60,00	-37,27	13,07	95,00	-47,93	29,01	85,00
5	60%	-70,81	25,50	60,00	-38,15	17,44	95,00	-50,45	28,62	85,00
6	70%	-50,62	37,14	60,00	-38,10	25,47	95,00	-48,42	30,10	85,00
7	80%	-45,08	31,65	60,00	-43,79	15,47	95,00	-53,80	23,43	85,00

Another important parameter of the study is the control distance, which is taken as 500, 750, 1000, 1250, and 1500 meters. At each incident scenario, CAVs are utilized in the control mechanism. The point at which CAVs are first instructed is determined as the point, which is a control distance upstream from the shockwave boundary. In Table 3.13, improvements due to different control distances and different CAV penetration rates can be observed. Results given in Table 3.13 indicate that each control distance provides noticeable improvements at each CAV market penetration rate except at 10%. It is also observed that, as the control distance increases, congestion improvements also increase. This improvement is related to the fact that high control distance means the control starting farther from the incident location. However, this might also result in the under utilization of the network.

Table 3.13. Performance of SWSCAV for Each Control Distance

CV	**500m K>38 Mean**	**500m K>38 Std Dev**	**500m # of Cases**	**750m K>38 Mean**	**750m K>38 Std Dev**	**750m # of Cases**	**1000m K>38 Mean**	**1000m K>38 Std Dev**	**1000m # of Cases**
10%	-15,83	46,43	48,00	-16,87	43,65	48,00	-19,22	41,92	48,00
20%	-29,39	36,15	48,00	-30,49	33,28	48,00	-33,55	30,82	48,00
30%	-28,97	36,12	48,00	-32,33	33,76	48,00	-34,04	31,43	48,00
40%	-36,61	33,41	48,00	-39,92	31,62	48,00	-43,11	33,47	48,00
50%	-43,97	36,30	48,00	-45,62	33,50	48,00	-48,08	31,63	48,00
60%	-47,10	27,96	48,00	-49,35	26,47	48,00	-49,92	28,52	48,00
70%	-40,31	34,79	48,00	-42,66	31,91	48,00	-47,35	29,85	48,00
80%	-44,26	24,72	48,00	-43,97	24,52	48,00	-48,16	23,48	48,00
CV	**1250m K>38 Mean**	**1250m K>38 Std Dev**	**1250m # of Cases**	**1500m K>38 Mean**	**1500m K>38 Std Dev**	**1500m # of Cases**			
10%	-21,90	39,41	48,00	-22,08	40,80	48,00			
20%	-36,13	30,58	48,00	-34,70	31,70	48,00			
30%	-37,35	27,98	48,00	-40,59	30,17	48,00			
40%	-40,62	30,61	48,00	-45,40	31,64	48,00			
50%	-50,29	27,54	48,00	-52,18	30,44	48,00			
60%	-51,85	28,17	48,00	-55,12	24,44	48,00			
70%	-46,24	28,21	48,00	-47,87	29,10	48,00			
80%	-49,78	22,53	48,00	-52,12	22,41	48,00			

Line charts of density and speed changes are provided in Figure 3.15. Analyzing Fig. 3.15., it is observed that CAV penetration rates higher than 40% provide lower densities in the case of an incident. This shows that high CAV rates improve congestions by stabilizing the traffic flow. Checking Fig. 3.16., it is seen that high CAV market penetration rates, such as 50-80%, do not provide as many changes in speeds as it does in density changes. However, due to the early and sharp decrease in speeds at high CAV rates, speed differences in the critical region are reduced and the traffic flow is homogenized. By the reduced speed differences, delays faced in the critical region mitigates and effects of shockwaves also reduce. On the other hand, in both Fig 3.15 and Fig 3.16, it is observed that the recovery after the incident location is much faster and more efficient at high CAV penetration rates. This reduces the impact of the incident on the overall network rather than just improving the critical region.

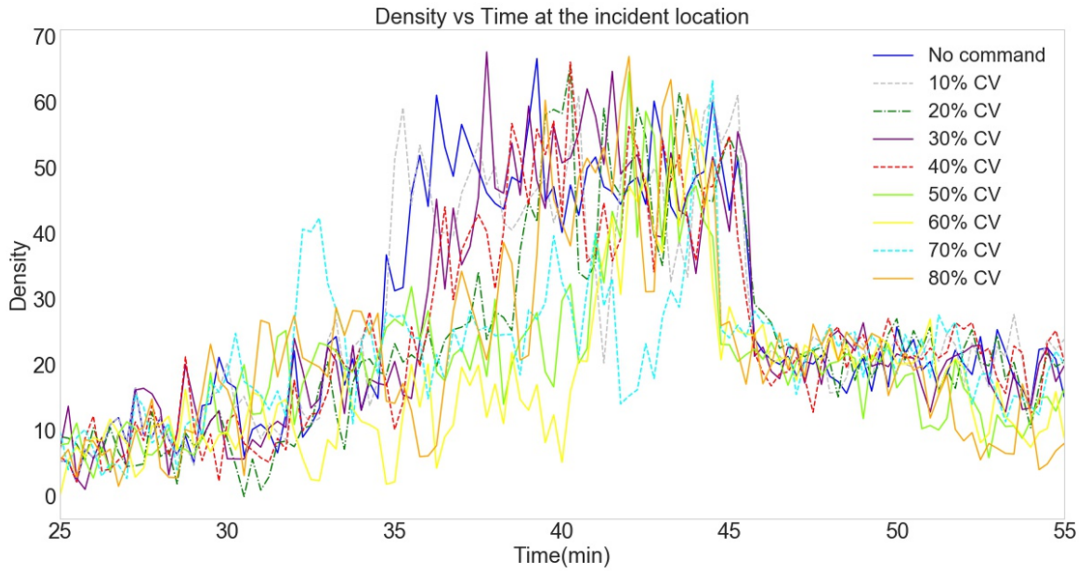

Figure 3.15. Density vs Time at the Incident Location

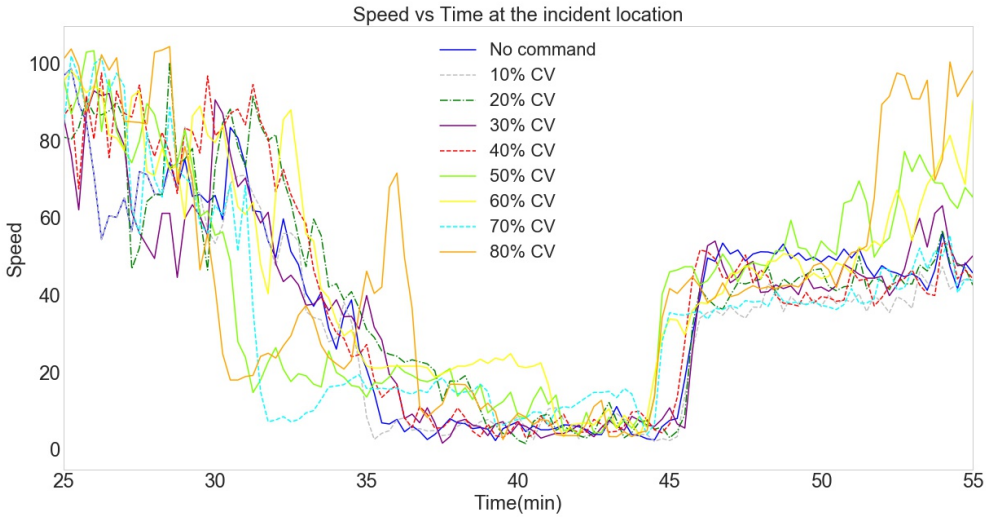

Figure 3.16. Speed vs Time at the Incident Location

3.1.10. Heatmaps

Fig. 3.17 and 3.18 provide the heatmaps of a base and controlled method of the same scenario. Comparing Fig. 3.17 and Fig. 3.18, it is observed that the controlled method distributes the density over time, which reduces the severity of the congestions present in the critical region. Both heatmaps contain a backward forming shockwave and a frontal stationary shockwave, which is the incident. After the incident location, a backward recovery shockwave is present. In the comparison of the heatmaps, it is seen that the controlled method reduces shockwave length, mitigates the shockwave's congestion severity, and distributes the severe congestions over time rather than having highly congested areas for less duration. These improvements provide fewer delays and fewer stop-and-go motions.

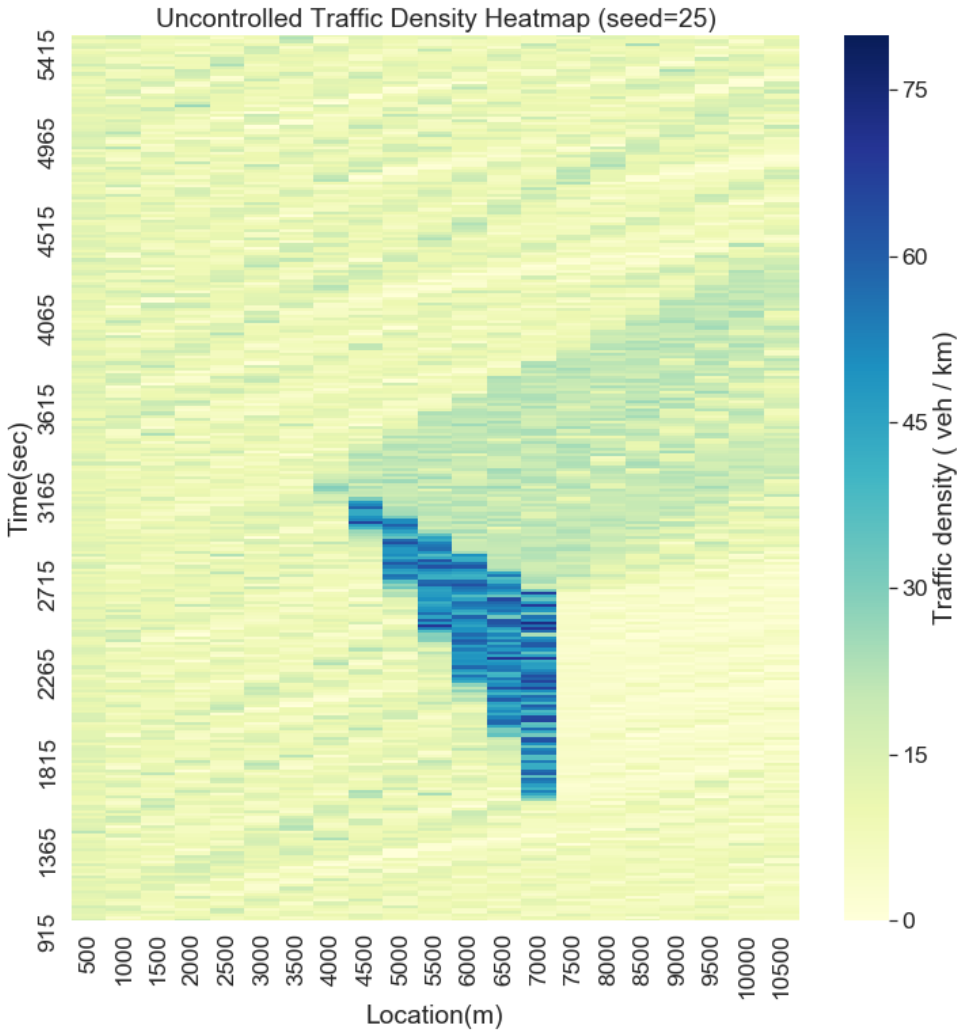

Figure 3.17. Uncontrolled Traffic Density Heatmap (seed=25)

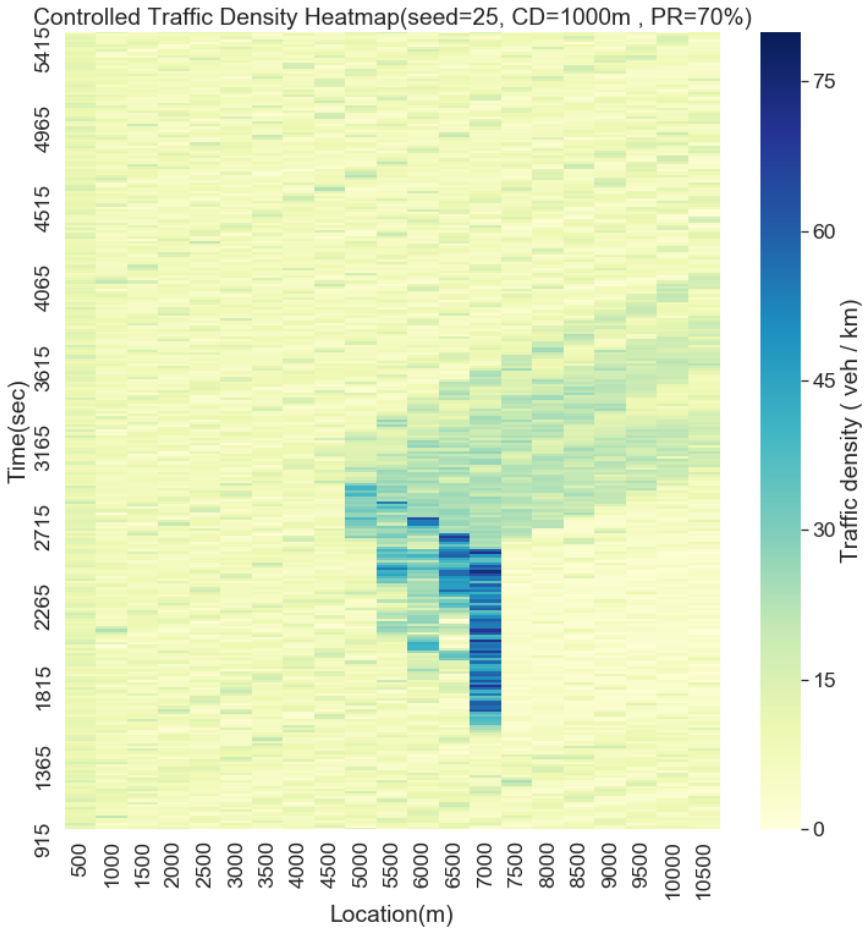

Figure 3.18. Controlled Traffic Density Heatmap(seed=25, CD=1000m, PR=70%)

3.1.11. Comparison with LCS and VSL

Lane control signals (LCS) and variable speed limits (VSL) are two widely used traffic management systems, which mainly aim to increase the traffic efficiency and safety aspect of the traffic in the case of an incident. The level of improvements of both management methods varies according to the compliance rate of the drivers. In the controlled method, LCS and VSL are simulated in the same environment to be able to compare them more accurately.

Table 3.14. Comparison of SWSCAV with Other Traffic Management Methods

Features	**Base**	**Uncontrolled**	**LCS**	**VSL**	**Controlled**	**Predicted**
K > 38(%)	3.81	-8.70	-7.53	-13.73	-18.04	-40.33
K > 28(%)	4.24	-12.13	-1.43	-13.10	-11.16	-28.93
Overall Avg. K	12.19	-10.37	-7.76	-10.70	-10.01	-12.08
Overall Avg. Speeds (km/hour)	64.68	12.04	9.97	11.97	11.07	11.21
Shockwave duration (min)	27.25	27.25	27.25	27.25	27.25	27.25
Shockwave length (meter)	3000	3000	3000	3000	3000	3000
In CR K > 38 (%)	35.71	-7.64	-6.18	-12.73	-17.09	-40.00
In CR K > 28 (%)	39.48	-11.84	-1.32	-12.17	-10.20	-27.96
In CR Avg. Speeds(km/hour) (%)	38.59	14.53	5.67	15.43	6.74	3.46

Table 3.14, Table 3.7, and Table 3.9 are the results of the same scenarios, which have the variables of 1000 meters control distance and 40% CAV percentage. In Table 3.14, it is seen that the controlled method improves the critical region better than any other method present by reducing densities at a higher percentage. Even though VSL has better results in average speeds, density reductions due to the controlled method carry bigger importance in relieving the critical region. It is also possible to observe that LCS does not provide as much when compared to VSL and controlled methods due to low-density reductions and speed increases. Even the uncontrolled method, which is having unmanaged CAVs in the system, performs better than LCS in means of both density reductions and speed improvements.

3.1.12. Simulation Results of Predicted Control Method

Table 3.15. Performance of SWSCAV for Each Incident Duration

Scenario	**CAV**	**10-15 K>38 Mean**	**10-15 K>38 Std Dev**	**Short Duration # of Scenarios**	**15-20 K>38 Mean**	**15-20 K>38 Std Dev**
0	10%	-34.58	29.23	85	-38.95	25.91
1	20%	-45.10	35.05	85	-27.92	26.57
2	30%	-47.37	33.49	85	-27.68	30.07
3	40%	-54.91	23.88	85	-49.19	23.40
4	50%	-63.06	18.95	85	-50.34	23.45
5	60%	-60.69	27.49	85	-57.77	18.17
6	70%	-63.03	20.94	85	-44.39	27.94
7	80%	-62.01	20.88	85	-55.37	15.00
Scenario	**CAV**	**Moderate Duration # of Scenarios**	**20-25 K>38 Mean**	**20-25 K>38 Std Dev**	**Long Duration # of Scenarios**	
0	10%	65	-4.54	59.51	90	
1	20%	65	-21.16	33.24	90	
2	30%	65	-20.04	42.36	90	
3	40%	65	-41.14	31.10	90	
4	50%	65	-59.25	35.36	90	
5	60%	65	-47.83	30.18	90	
6	70%	65	-34.22	25.18	90	
7	80%	65	-40.00	25.51	90	

In Table 3.15, standard deviation and mean values of the changes in density, which are bigger than the threshold of 38 veh/km, according to different incident durations and changing CAV percentages are present. For the short duration incidents that take around 10 to 15 minutes, it is observed that 50% CAV is the optimum case since the biggest decrease in mean values and the lowest increase in standard deviation values

is seen at this CAV percentage value. For the moderate duration incidents that take around 15 to 20 minutes, 60% CAV is seen to be the optimum case due to the mean and standard deviation values and for the long duration incidents, which take around 20 to 25 minutes, 50% CAV is seen to be the best case.

Table 3.16. Performance of Predicted SWSCAV for Each Penetration Rate

Scenario	**Features**	**10%**	**20%**	**30%**	**40%**	**50%**	**60%**	**70%**	**80%**
0	K>38 Mean	-24.50	-31.47	-31.79	-48.20	-58.18	-55.08	-47.18	-51.96
1	K>38 Std Dev	45.18	33.79	38.04	27.25	27.66	26.95	27.46	23.42
2	K>28 Mean	-23.82	-30.73	-31.31	-47.29	-56.42	-54.86	-45.91	-50.88
3	K¿28 Std Dev	37.20	29.24	35.21	23.99	24.56	21.80	26.46	19.50
4	Scenario Number	240	240	240	240	240	240	240	240

In Table 3.16, standard deviation and mean values of the changes in density, which are bigger than the thresholds of both 28 and 38 veh/km, according to changing CAV percentages are present. Unlike Table 3.16, the incident duration is not a variable in this table, so the optimum CAV percentage is observed regardless of the incident duration variable. Analyzing the table, it is seen that 50% CAV penetration rate is the optimum case for the predicted method because for both 'K>38' and 'K>28' mean and standard deviation rows, the biggest decrease in mean percent density change values are observed at 50% CAV penetration rate and one of the lowest standard deviation increase is seen again at 50% CAV penetration rate.

Table 3.17. Performance of SWSCAV for Each Incident Lane

Scenario	**CAV**	**Right K>38 Mean**	**Right K>38 Std Dev**	**Right # Shockwave Scenarios**	**Middle K>38 Mean**	**Middle K>38 Std Dev**	**Middle # Shockwave Scenario**
0	10%	-20.95	68.20	60	-25.01	17.36	95
1	20%	-32.66	35.86	60	-31.81	23.43	95
2	30%	-34.44	48.16	60	-41.60	19.69	95
3	40%	-59.00	36.79	60	-43.66	14.71	95
4	50%	-88.71	12.63	60	-50.47	13.03	95
5	60%	-62.70	25.66	60	-55.00	16.39	95
6	70%	-41.64	34.55	60	-49.75	18.15	95
7	80%	-45.93	28.95	60	-54.91	12.25	95
Scenario	**CAV**	**Left K>38 Mean**	**Left K>38 Std Dev**	**Left # Shockwave Scenario**			
0	10%	-26,43	46,82	85,00			
1	20%	-30,25	41,57	85,00			
2	30%	-18,94	42,12	85,00			
3	40%	-45,64	28,40	85,00			
4	50%	-45,25	31,17	85,00			
5	60%	-49,79	35,12	85,00			
6	70%	-48,20	30,12	85,00			
7	80%	-52,92	27,71	85,00			

In Table 3.17, mean and standard deviation values of the percent changes in densities bigger than the threshold 38 veh/km are shown according to variating CAV percentages and incident lanes. There are 105, 95 and 100 cases of incident scenarios for right, middle, and left lanes respectively, however the formation of the shockwave is not the case for each scenario just like it is stated in the discussion of the controlled method. Right lane incident cases having a low ratio of shockwave formation indicates that improving shockwaves that are due to right lane incidents is much easier than middle and left lane incident cases. High mean and low standard deviation values of the right lane incident cases compared with the other incident lane cases support this idea. Analyzing the table for the right lane case, it is seen that 50% CAV penetration shows 88.71% decrease in mean percent density value and 12.63% increase in standard

deviation value, which is a great improvement compared to the results of both the controlled method and other incident lane cases. For the middle and left incident lane cases, it is observed that 50% and 60% CAV penetration is the optimum case.

Table 3.18. Performance of SWSCAV for Each Control Distance

Scenario	**CV**	**500m K>38 Mean**	**500m K>38 Std Dev**	**500m # Cases**	**750m K>38 Mean**	**750m K>38 Std Dev**	**750m # Cases**	**1000m K>38 Mean**	**1000m K>38 Std Dev**	**1000m # Cases**
0	10%	-21.06	46.88	48	-20.14	48.15	48	-28.69	45.81	48
1	20%	-27.76	36.85	48	-29.24	32.97	48	-36.16	32.99	48
2	30%	-25.02	42.60	48	-29.26	39.51	48	-36.53	32.03	48
3	40%	-44.75	29.93	48	-47.29	26.43	48	-52.17	26.52	48
4	50%	-54.70	31.15	48	-54.85	30.99	48	-60.86	27.34	48
5	60%	-50.42	29.69	48	-52.99	27.09	48	-59.40	24.25	48
6	70%	-43.22	29.19	48	-41.88	29.36	48	-51.72	26.42	48
7	80%	-46.72	24.35	48	-49.87	23.34	48	-56.44	23.29	48
Scenario	**CV**	**1250m K>38 Mean**	**1250m K>38 Std Dev**	**1250m # Cases**	**1500m K>38 Mean**	**1500m K>38 Std Dev**	**1500m # Cases**			
0	10%	-27.19	38.77	48	-25.41	46.98	48			
1	20%	-29.93	34.34	48	-34.27	32.27	48			
2	30%	-29.76	42.27	48	-38.36	32.35	48			
3	40%	-47.05	27.74	48	-49.71	26.00	48			
4	50%	-58.90	25.61	48	-61.61	22.62	48			
5	60%	-55.00	27.97	48	-57.58	25.60	48			
6	70%	-47.58	27.05	48	-51.49	24.60	48			
7	80%	-51.75	23.38	48	-55.01	22.38	48			

Another important variable of the study is the control distance from the upstream boundary of the shockwave at which CAVs are being instructed. In Table 3.18, the effects of control distances with changing CAV penetration rates are given. Comparing each control distance depending on the mean and standard deviation values, it is observed that 1250 meters are the most optimum control distance since at the best CAV penetration rate, which is 50%, the highest mean value decrease and lowest standard

deviation increase is seen at this control distance. Even at CAV penetration rates different than 50%, a control distance of 1250 meters shows the best or second-best results compared to other control distances.

3.1.13. Lineplots

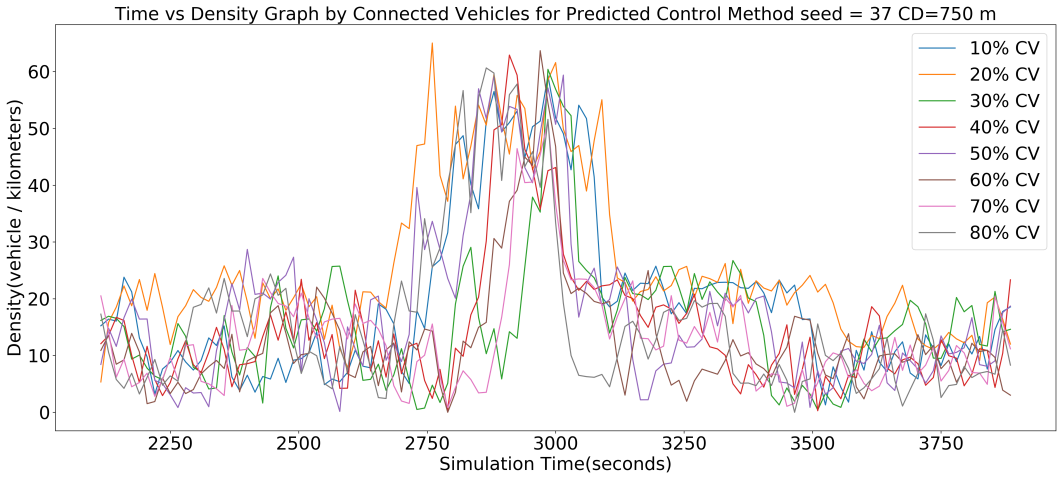

Figure 3.19. Time vs Density Graph 750m

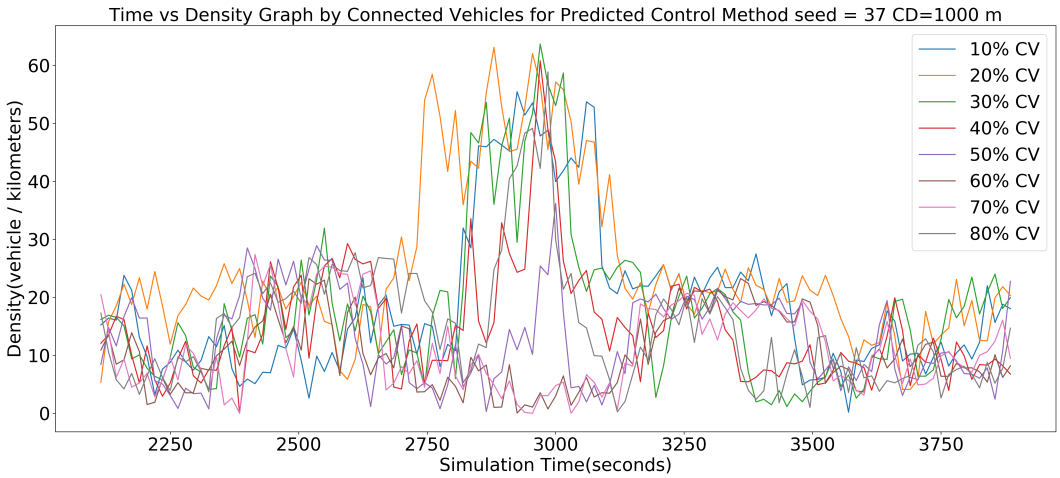

Figure 3.20. Time vs Density Graph 1000m

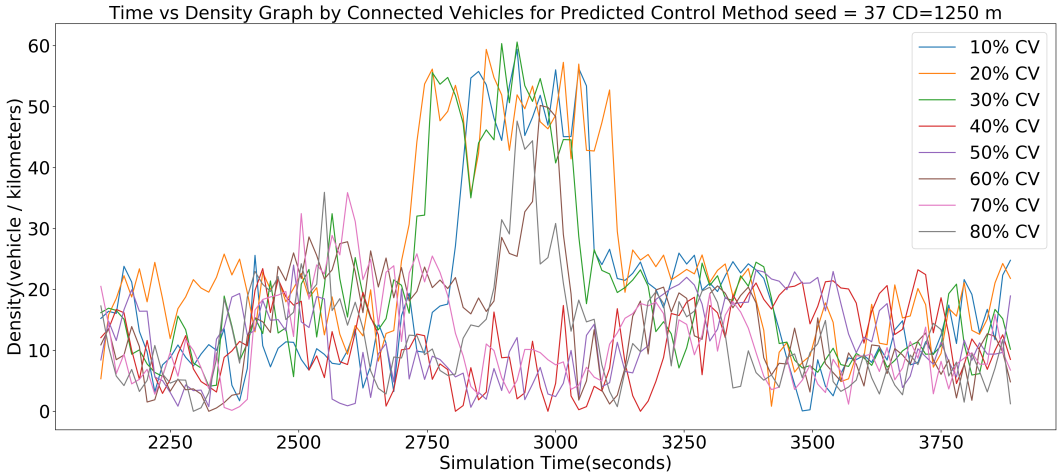

Figure 3.21. Time vs Density Graph 1250m

In Fig 3.19, 3.20 and 3.21., line plots of density vs. time for different control distances, which are 750, 1000 and 1250 meters, and different CAV percentages are provided. Comparing these plots, it is observed that, best density improvements are seen at the control distance of 1250 meters due to the lowered densities in the shockwave area. By the reduction in densities in the critical region, it is possible to say that delays and stop-and-go motion faced in the critical region are reduced. It is also observed that, at the most optimum control distance, which is 1250 meters, CAV penetration rates of 40%, 50%, and 60% outperform other penetration rates. These findings support the idea of the most optimum case for the predicted control method being the 50% CAV penetration rate at a control distance of 1250 meters.

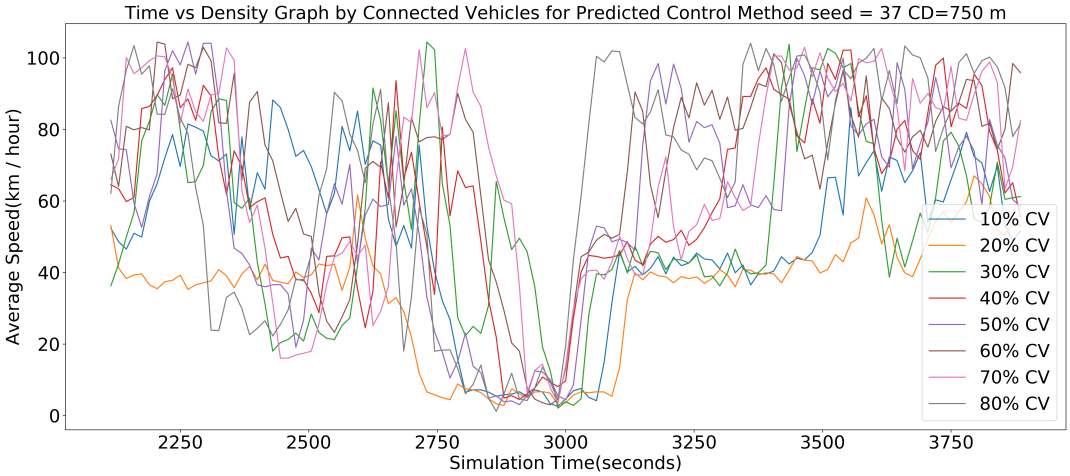

Figure 3.22. Time vs Speed Graph 750m

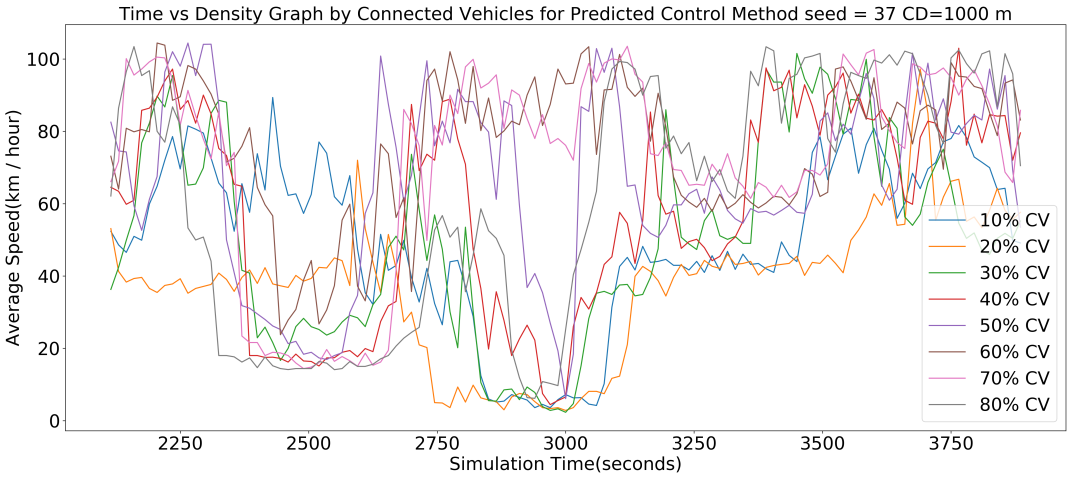

Figure 3.23. Time vs Speed Graph 1000m

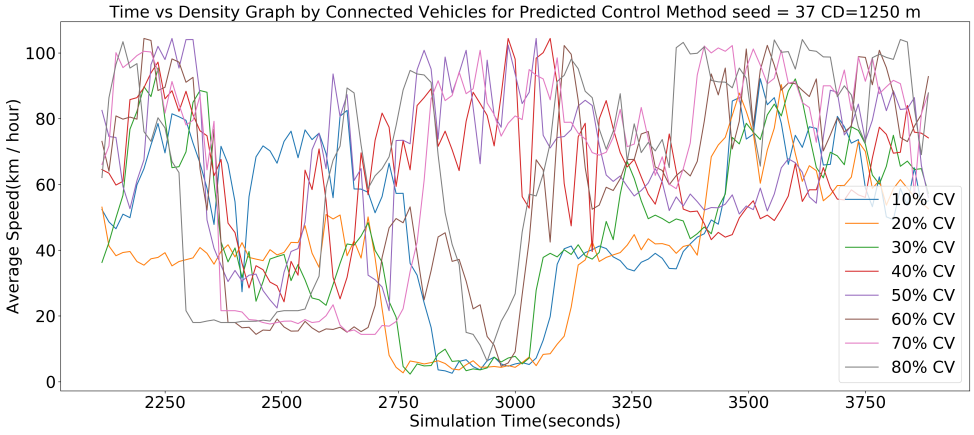

Figure 3.24. Time vs Speed Graph 1250m

In Fig. 3.22, 3.23 and 3.24, line plots of speed vs. time for different control distances and CAV percentages are provided. Comparing these line plots, it is seen that at the control distance of 750 meters, there are sharp speed increases and decreases, which may increase the delays faced, safety issues, and also decrease fuel efficiency. As the control distance increases, it is seen that the first sharp decrease in speeds is taking place at a farther location from the incident and there are not many sharp speed changes after the first decrease, which reduces speed differences, homogenize the traffic, increases the safety of the drivers, and increase fuel efficiency due to reduced stop-and-go motions faced. Best speed improvements related to the homogenization of the speeds are observed at 1250 meters. Analyzing the CAV percentage trends at the control distance of 1250 meters, it is seen that the CAV penetration rates of 40%, 50%, and 70% show the best improvements, which supports the selection of 50% CAV penetration as the most optimum one.

3.1.14. Heatmaps

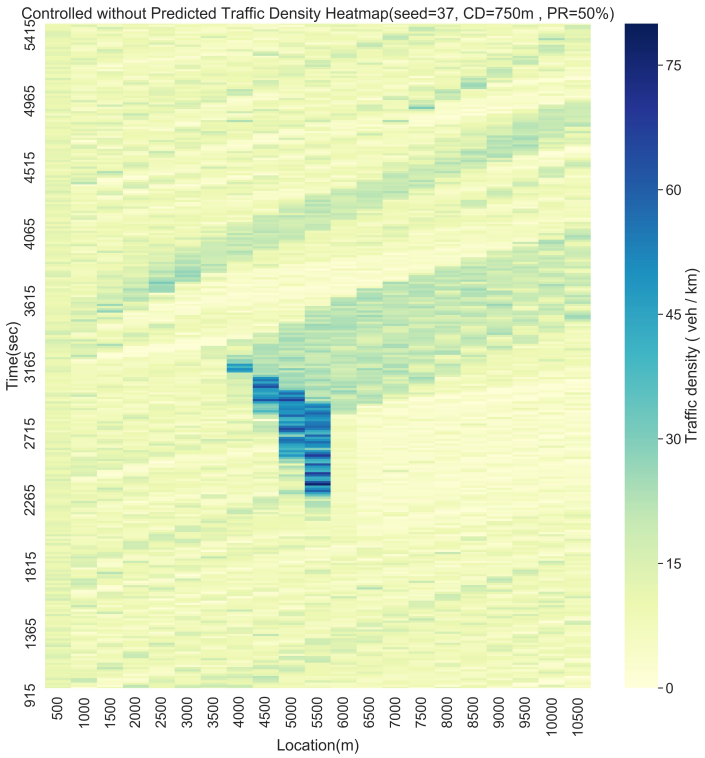

Figure 3.25. Controlled Traffic Density Heatmap(seed=37 CD=750m PR=50%)

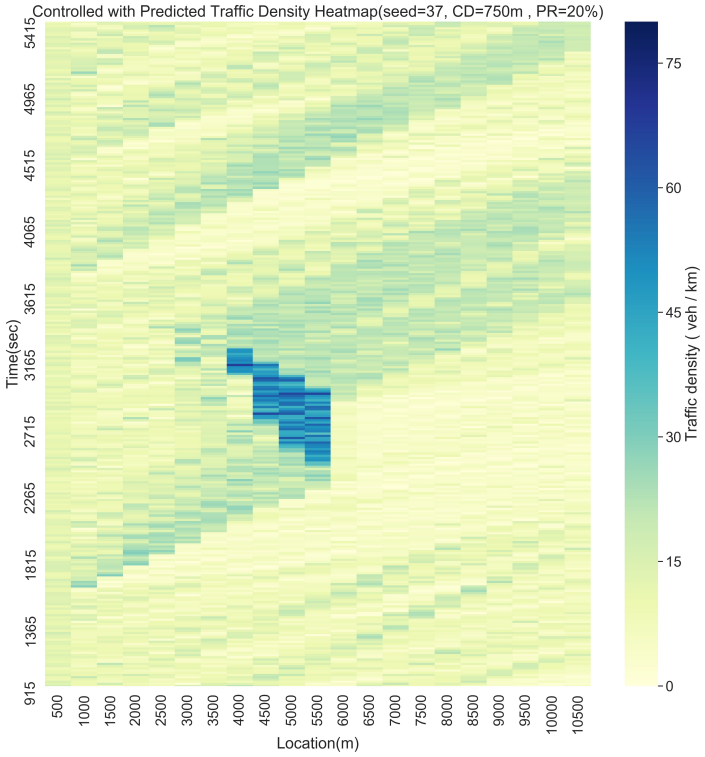

Figure 3.26. Controlled with Predicted Traffic Density Heatmap(seed=37 CD=750m PR=20%

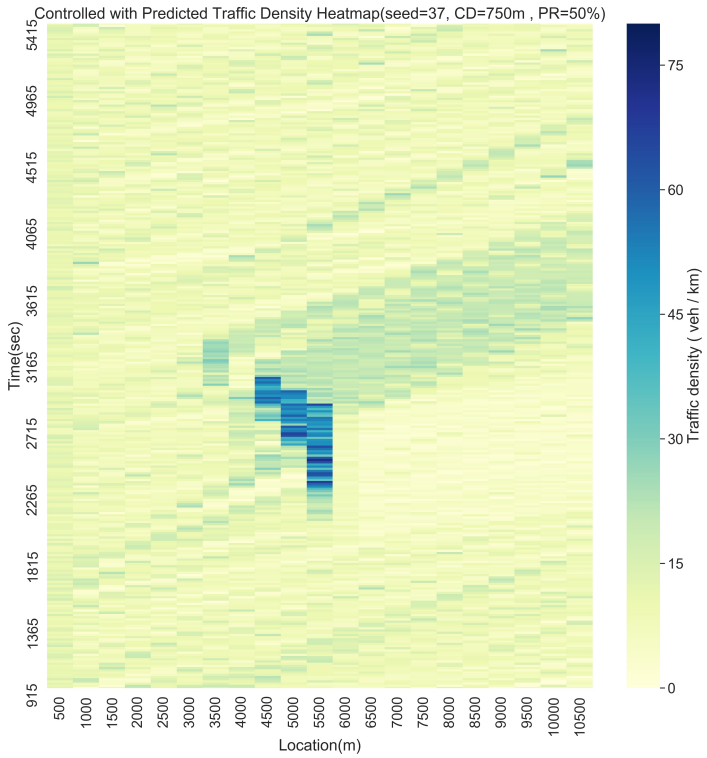

Figure 3.27. Controlled with Predicted Traffic Density Heatmap(seed=37 CD=750m PR=50%

In Fig.3.25, 3.26 and 3.27, three different heatmaps are present. Fig. 3.25 is the heatmap of a base scenario where Fig. 3.26 and Fig.3.27 are the heatmaps of the results of the predicted control method with different CAV penetration rates. Fig. 3.26 contains 20% CAV and Fig. 3.27 contains 50% CAV. All three heatmaps are constructed according to the same control distance, which is 750 meters. Comparing the heatmaps, it is observed that the predicted control method reduces densities and improves the critical region. Shockwave distances and shockwave durations of the 500 meters intervals within the critical region are significantly reduced. This shows that the lengths of the queues, which are due to the incident are lowered and stop-and-go motion within the shockwave area is reduced. It is also seen that 50% CAV outperforms the

20% CAV case by the reduction in shockwave length in the critical region and better mitigation of highly dense areas.

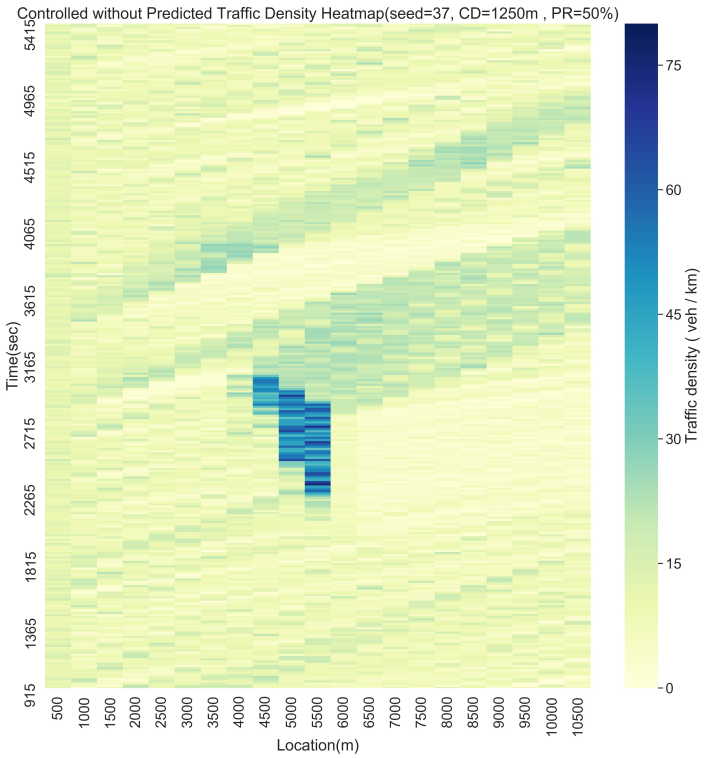

Figure 3.28. Controlled Traffic Density Heatmap(seed=37 CD=1250m PR=50%)

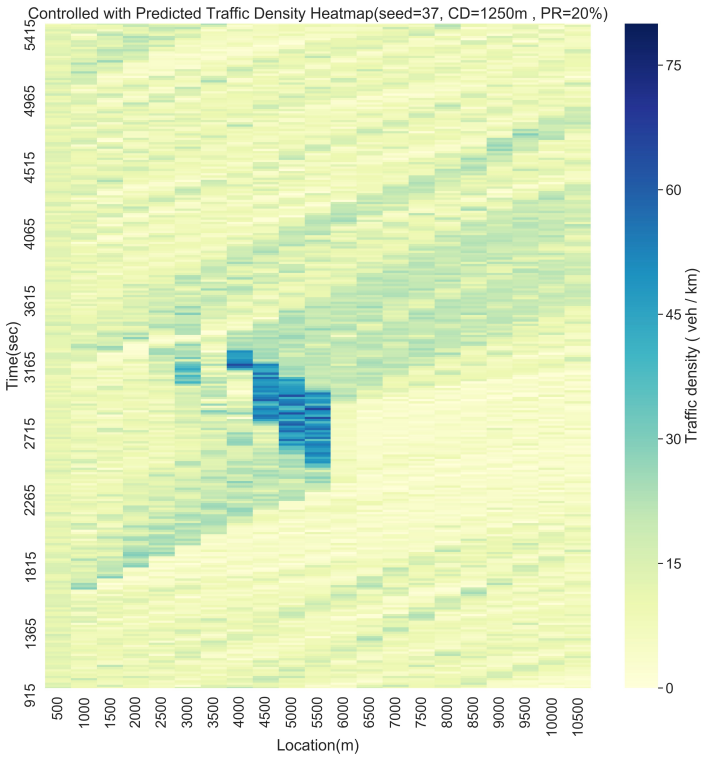

Figure 3.29. Controlled with Predicted Traffic Density Heatmap(seed=37 CD=1250m PR=20%

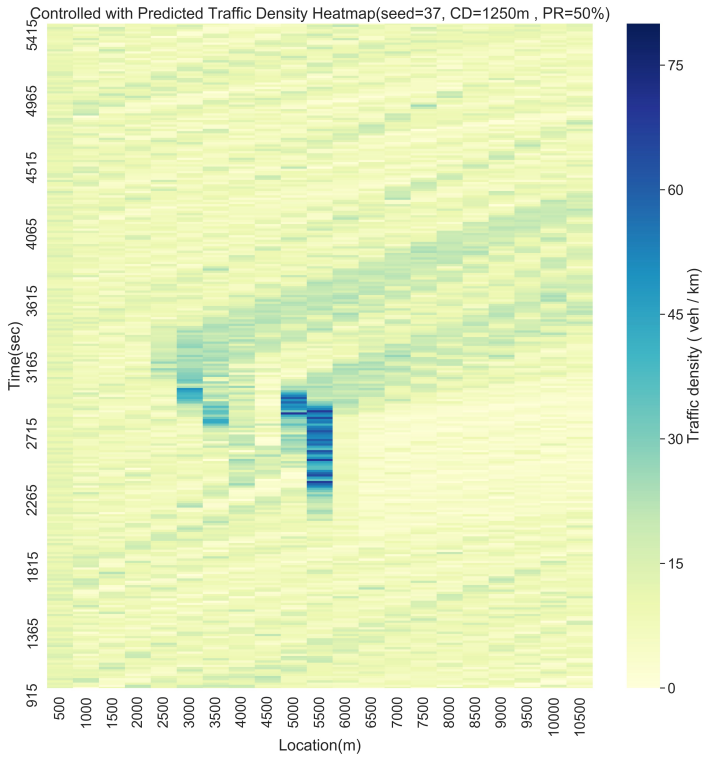

Figure 3.30. Controlled with Predicted Traffic Density Heatmap(seed=37 CD=1250m PR=50%

In Fig 3.28, 3.29 and 3.30, heatmaps of a base scenario and two predicted control method is present. Heatmaps of the predicted control method are constructed based on the control distance of 1250 meters, which is the optimum control distance for the method. Fig 3.29 and Fig 3.30 differ on the CAV percentage being 20% and 50% respectively. Comparing these scenarios, its possible to see that the predicted control method mitigates high-density areas very successfully, and also, this method starts the management of the shockwave from a farther distance from the incident, which creates small highly dense areas upstream. Management starting from a farther point homogenizes the critical region to a better extent. Comparing Fig 3.27 and Fig 3.30, it is easily seen that the optimum control distance being 1250 meters is an accurate

analysis due to the heatmap, present at Fig 3.30, having less highly congested areas and more stable traffic.

3.1.15. Comparison of Predicted Control Method with LCS and VSL

Table 3.19. Comparison of Predicted Control Method with LCS and VSL

Scenario	**Features**	**Base**	**Uncontrolled-% Change**	**LCS-% Change**	**VSL-% Change**	**Controlled-% Change**	**Predicted-% Change**
0	K > 38(%)	3.81	-28.62	-28.26	-27.68	-35.06	-43.34
1	K > 28(%)	4.24	-28.91	-18.99	-26.05	-25.72	-42.14
2	Overall Avg. K	12.19	-17.43	-13.37	-16.32	-16.44	-17.10
3	Overall Avg. Speed (km/hour)	64.68	22.05	18.60	21.94	21.15	19.85
4	Shockwave duration (min)	27.25	27.25	27.25	27.25	27.25	27.25
5	Shockwave length (meter)	3000	3000	3000	3000	3000	3000
6	In CR K > 38 (%)	35.71	-29.45	-29.09	-28.73	-36.00	-44.00
7	In CR K > 28 (%)	39.48	-29.93	-20.39	-27.30	-26.97	-42.76
8	In CR Avg. Speeds(km/hour) (%)	38.59	37.69	31.36	36.06	27.91	18.66

In Table 3.19, the results of a simulation with the variables of 1250 meters control distance and 50% CAV penetration rate, which are the optimum values of the variables for the predicted control method, are present. Comparing the results of LCS, VSL, and predicted control method, it is possible to observe that the predicted control method improves both highly dense areas and the overall density of the network to a better extent. However, improvements regarding the critical region are more important when comparing these management methods since these methods are used to improve the critical region in the case of an incident. Comparing the results of the changes in the critical region, it is seen that the predicted control method is better in controlling the shockwave due to the higher percent changes in the areas, where density is bigger than the thresholds of 28 and 38 veh/km. These findings can also be interpreted as the

predicted control method reduces the stop-and-go motions in the critical region and stabilizes the traffic better than LCS and VSL.

Table 3.20. Comparison of the Predicted and Unpredicted SWSCAV by Incident Duration

Control Method	Scenario	CAV	10-15 K>38 Mean	10-15 K>38 Std Dev	Short Duration # of Scenarios	15-20 K>38 Mean	15-20 K>38 Std Dev	Moderate Duration # of Scenarios
Predicted Control Method	0	10%	-34.58	29.23	85	-38.95	25.91	65,00
	1	20%	-45.10	35.05	85	-27.92	26.57	65,00
	2	30%	-47.37	33.49	85	-27.68	30.07	65,00
	3	40%	-54.91	23.88	85	-49.19	23.40	65,00
	4	50%	-63.06	18.95	85	-50.34	23.45	65,00
	5	60%	-60.69	27.49	85	-57.77	18.17	65,00
	6	70%	-63.03	20.94	85	-44.39	27.94	65,00
	7	80%	-62.01	20.88	85	-55.37	15.00	65,00
	Scenario	**CAV**	**20-25 K>38 Mean**	**20-25 K>38 Std Dev**	**Long Duration # of Scenarios**			
	0	10%	-4.54	59.51	90			
	1	20%	-21.16	33.24	90			
	2	30%	-20.04	42.36	90			
	3	40%	-41.14	31.10	90			
	4	50%	-59.25	35.36	90			
	5	60%	-47.83	30.18	90			
	6	70%	-34.22	25.18	90			
	7	80%	-40.00	25.51	90			
Controlled Method	**Scenario**	**CAV**	**10-15 K>38 Mean**	**10-15 K>38 Std Dev**	**Short Duration # of Scenarios**	**15-20 K>38 Mean**	**15-20 K>38 Std Dev**	**Moderate Duration # of Scenarios**
	0	10%	-32,31	39,85	85,00	-24,31	29,81	65,00
	1	20%	-39,80	32,18	85,00	-34,29	33,68	65,00
	2	30%	-43,81	30,53	85,00	-28,61	26,63	65,00
	3	40%	-51,70	28,82	85,00	-45,90	23,13	65,00
	4	50%	-54,74	25,19	85,00	-47,31	21,17	65,00
	5	60%	-52,55	27,83	85,00	-49,42	24,03	65,00
	6	70%	-55,73	29,05	85,00	-53,83	30,76	65,00
	7	80%	-54,06	24,49	85,00	-52,99	17,03	65,00
	Scenario	**CAV**	**20-25 K>38 Mean**	**20-25 K>38 Std Dev**	**Long Duration # of Scenarios**			
	0	10%	-3,08	46,97	90,00			
	1	20%	-24,67	31,92	90,00			
	2	30%	-30,37	35,14	90,00			
	3	40%	-27,71	35,81	90,00			
	4	50%	-42,21	41,62	90,00			
	5	60%	-49,79	28,54	90,00			
	6	70%	-42,63	29,22	90,00			
	7	80%	-37,76	23,62	90,00			

In Table 3.20, mean and standard deviation values of the percent change in densities bigger than the threshold 38 for each CAV percentage are present for short, moderate, and long duration incident scenarios. Comparing the optimum cases for each control method, which are 50% for the predicted control method and 70% for the controlled method, it is observed that in many of the scenarios, the predicted control method outperforms the controlled method with higher reductions in mean values and lower increases in standard deviation values. Analyzing short and moderate incident duration, it is seen that the predicted control method improves the critical region to a better extent at almost every CAV penetration rate. However, at long-duration incidents, the predicted control method shows better performance at only 40% and 50% CAV penetration rates, which are near around the optimum CAV percentage rate of the method. These findings indicate that the implementation of the predicted control method at short and moderate incident duration cases is more appropriate regardless of the CAV percentage, but the application of the predicted control method at long incident duration cases is dependent on the CAV percentage.

Table 3.21. Comparison of Predicted and Unpredicted SWSCAV by Penetration Rate

Control Method	**Scenario**	**Features**	**10%**	**20%**	**30%**	**40%**	**50%**	**60%**	**70%**	**80%**
Predicted Control Method	0	K>38 Mean	-24.50	-31.47	-31.79	-48.20	-58.18	-55.08	-47.18	-51.96
	1	K>38 Std Dev	45.18	33.79	38.04	27.25	27.66	26.95	27.46	23.42
	2	K>28 Mean	-23.82	-30.73	-31.31	-47.29	-56.42	-54.86	-45.91	-50.88
	3	K>28 Std Dev	37.20	29.24	35.21	23.99	24.56	21.80	26.46	19.50
	4	Scenario Number	240	240	240	240	240	240	240	240
Controlled Method	0	K>38 Mean	2,04	-4,45	-1,93	-9,00	-5,97	-14,77	-16,31	-16,14
	1	K>38 Std Dev	32,81	22,64	20,59	26,80	32,48	12,02	20,79	14,80
	2	K>28 Mean	2,19	-2,62	2,31	-9,59	-8,23	-16,15	-2,95	-18,61
	3	K>28 Std Dev	33,81	17,35	23,94	19,55	29,08	10,30	26,02	15,67
	4	Scenario Number	161,00	109,00	93,00	79,00	48,00	51,00	61,00	49,00

In Table 3.21, the impact of CAV percentage on both control methods is investigated. The effect of the CAV penetration rate is analyzed on the mean and standard deviation values of the changes in percent densities bigger than the thresholds of 28 and 38. Unlike Table 15, this table does not take incident durations into account, so

average results are present. Comparing the controlled method and the predicted control method, it is observed that, predicted control method outperforms the controlled method at each CAV percentage since mean values of the decrease in density values bigger than 38 and 28 are higher when the predicted control method is applied. It is also seen that the standard deviation of the changes shows better results in controlled method results due to lower values, however, changes in mean values are comparatively more significant. Therefore, predicted control method results indicate better use of the predicted control method when CAV percentage dependent results are compared.

Table 3.22. Comparison of Predicted and Unpredicted SWSCAV by Incident Lane

Control Method	**Scenario**	**CAV**	**Right K>38 Mean**	**Right K>38 Std Dev**	**Right # of Cases**	**Middle K>38 Mean**	**Middle K>38 Std Dev**	**Middle # of Cases**
	0	10%	-20,95	68,20	60,00	-25,01	17,36	95,00
	1	20%	-32,66	35,86	60,00	-31,81	23,43	95,00
	2	30%	-34,44	48,16	60,00	-41,60	19,69	95,00
	3	40%	-59,00	36,79	60,00	-43,66	14,71	95,00
	4	50%	-88,71	12,63	60,00	-50,47	13,03	95,00
	5	60%	-62,70	25,66	60,00	-55,00	16,39	95,00
	6	70%	-41,64	34,55	60,00	-49,75	18,15	95,00
	7	80%	-45,93	28,95	60,00	-54,91	12,25	95,00
Predicted Control Method	**Scenario**	**CAV**	**Left K>38 Mean**	**Left K>38 Std Dev**	**Left # of Cases**			
	0	10%	-26,43	46,82	85,00			
	1	20%	-30,25	41,57	85,00			
	2	30%	-18,94	42,12	85,00			
	3	40%	-45,64	28,40	85,00			
	4	50%	-45,25	31,17	85,00			
	5	60%	-49,79	35,12	85,00			
	6	70%	-48,20	30,12	85,00			
	7	80%	-52,92	27,71	85,00			
	Scenario	**CAV**	**Right K>38 Mean**	**Right K>38 Std Dev**	**Right # of Cases**	**Middle K>38 Mean**	**Middle K>38 Std Dev**	**Middle # of Cases**
	0	10%	-12,98	60,85	60,00	-14,03	18,82	95,00
	1	20%	-45,74	38,29	60,00	-24,32	20,90	95,00
	2	30%	-44,42	30,36	60,00	-32,08	26,09	95,00
	3	40%	-46,57	48,68	60,00	-32,74	17,47	95,00
	4	50%	-65,20	46,50	60,00	-37,27	13,07	95,00
Controlled Method	5	60%	-70,81	25,50	60,00	-38,15	17,44	95,00
	6	70%	-50,62	37,14	60,00	-38,10	25,47	95,00
	7	80%	-45,08	31,65	60,00	-43,79	15,47	95,00
	Scenario	**CAV**	**Left K>38 Mean**	**Left K>38 Std Dev**	**Left # of Cases**			
	0	10%	-29,31	43,77	85,00			
	1	20%	-32,67	37,18	85,00			
	2	30%	-30,64	37,58	85,00			
	3	40%	-46,68	27,98	85,00			
	4	50%	-47,93	29,01	85,00			
	5	60%	-50,45	28,62	85,00			
	6	70%	-48,42	30,10	85,00			
	7	80%	-53,80	23,43	85,00			

In Table 3.22, mean and standard deviation values for each CAV percentage and incident lane scenario are present. Analyzing middle and left incident lane simulation results, it is observed that the predicted control method enhances the critical region better than the controlled method since the mean percent decrease in density values are better at each scenario and standard deviation values are similar, which makes the predicted control method a better choice. Checking the results of the right lane incident scenarios, the predicted control method outperformed the controlled method at only 40% and 50% CAV penetration rates. The same findings also apply for Table 3.15 short duration scenarios because comparing the results of each incident duration case, it is seen that improvement regarding the short duration case is very promising even at very low CAV percentages, so improving short duration incident scenarios is easier compared to other incident duration cases. Right lane scenarios and short incident duration scenarios have this in common and also, the fact that the controlled method shows better results at these scenarios, except for 40% and 50% cases, indicates that improving shockwaves, which are easy to deal with, can be solved by the controlled method more efficiently, whereas shockwaves, which are complicated and hard to deal with, can be improved by the implementation of predicted control method more efficiently.

Table 3.23. Comparison of Predicted and Unpredicted SWSCAV by Control Distance

Control Method	Scenario	CV	500m K>38 Mean	500m K>38 Std Dev	500m Cases	#	750m K>38 Mean	750m K>38 Std Dev	750m Cases	#	1000m K>38 Mean	1000m K>38 Std Dev	1000m Cases	#
Predicted Control Method	0	10%	-21.06	46.88	48		-20.14	48.15	48		-27.19	38.77	48	
	1	20%	-27.76	36.85	48		-29.24	32.97	48		-29.93	34.34	48	
	2	30%	-25.02	42.60	48		-29.26	39.51	48		-29.76	42.27	48	
	3	40%	-44.75	29.93	48		-47.29	26.43	48		-47.05	27.74	48	
	4	50%	-54.70	31.15	48		-54.85	30.99	48		-58.90	25.61	48	
	5	60%	-50.42	29.69	48		-52.99	27.09	48		-55.00	27.97	48	
	6	70%	-43.22	29.19	48		-41.88	29.36	48		-47.58	27.05	48	
	7	80%	-46.72	24.35	48		-49.87	23.34	48		-51.75	23.38	48	
	Scenario	**CV**	**1250m K>38 Mean**	**1250m K>38 Std Dev**	**1250m Cases**	**#**	**1500m K>38 Mean**	**1500m K>38 Std Dev**	**1500m Cases**	**#**				
	0	10%	-25.41	46.98	48		-28.69	45.81	48					
	1	20%	-34.27	32.27	48		-36.16	32.99	48					
	2	30%	-38.36	32.35	48		-36.53	32.03	48					
	3	40%	-49.71	26.00	48		-52.17	26.52	48					
	4	50%	-61.61	22.62	48		-60.86	27.34	48					
	5	60%	-57.58	25.60	48		-59.40	24.25	48					
	6	70%	-51.49	24.60	48		-51.72	26.42	48					
	7	80%	-55.01	22.38	48		-56.44	23.29	48					
Controlled Method	**Scenario**	**CV**	**500m K>38 Mean**	**500m K>38 Std Dev**	**500m Cases**	**#**	**750m K>38 Mean**	**750m K>38 Std Dev**	**750m Cases**	**#**	**1000m K>38 Mean**	**1000m K>38 Std Dev**	**1000m Cases**	**#**
	0	10%	-15,83	46,43	48		-16,87	43,65	48		-19,22	41,92	48	
	1	20%	-29,39	36,15	48		-30,49	33,28	48		-33,55	30,82	48	
	2	30%	-28,97	36,12	48		-32,33	33,76	48		-34,04	31,43	48	
	3	40%	-36,61	33,41	48		-39,92	31,62	48		-43,11	33,47	48	
	4	50%	-43,97	36,30	48		-45,62	33,50	48		-48,08	31,63	48	
	5	60%	-47,10	27,96	48		-49,35	26,47	48		-49,92	28,52	48	
	6	70%	-40,31	34,79	48		-42,66	31,91	48		-47,35	29,85	48	
	7	80%	-44,26	24,72	48		-43,97	24,52	48		-48,16	23,48	48	
	Scenario	**CV**	**1250m K>38 Mean**	**1250m K>38 Std Dev**	**1250m Cases**	**#**	**1500m K>38 Mean**	**1500m K>38 Std Dev**	**1500m Cases**	**#**				
	0	10%	-21,90	39,41	48		-22,08	40,80	48					
	1	20%	-36,13	30,58	48		-34,70	31,70	48					
	2	30%	-37,35	27,98	48		-40,59	30,17	48					
	3	40%	-40,62	30,61	48		-45,40	31,64	48					
	4	50%	-50,29	27,54	48		-52,18	30,44	48					
	5	60%	-51,85	28,17	48		-55,12	24,44	48					
	6	70%	-46,24	28,21	48		-47,87	29,10	48					
	7	80%	-49,78	22,53	48		-52,12	22,41	48					

In Table 3.23, improvements provided by the controlled method and predicted control method are presented with the variables of control distance and CAV percentage. It is seen that as the control distance decreases, the effectiveness of the methods also decreases. Analyzing the results of the predicted control method given in Table

3.23, it is seen that the best improvements on the shockwave are met at the control distance of 1250 meters because the highest mean decreases with comparatively low standard deviations are observed at this control distance. For the controlled method, the optimum control distance is observed to be the same, which is 1250 meters, due to the same reason. These findings finalize the selection of the optimum case for each method with the determination of the optimum control distances. The controlled method's optimum case is seen at the scenario with a control distance of 1250 meters and 70% CAV penetration rate, whereas the optimum case of the predicted control method is seen at the same control distance, but with the CAV penetration rate of 50%. In Tables 3.24 and 3.25, results of the simulations regarding the optimum cases of each method at the same seed are present.

Table 3.24. Scenario Control Distance=1250 Penetration Rate=50 Seed=4

Scenario	**Features**	**Base**	**Uncontrolled**	**LCS**	**VSL**	**Controlled**	**Predicted**
0	K > 38%	2.55	2.33	2.28	2.31	2.00	1.57
1	K > 28(%)	2.80	2.60	2.92	2.49	2.39	2.09
2	Overall Avg. K	11.59	10.18	10.62	10.05	10.07	10.14
3	Overall Avg. Speeds (km/hour)	61.52	76.30	75.30	78.01	77.18	75.59
4	Shockwave duration (min)	22.50	22.50	22.50	22.50	22.50	22.50
5	Shockwave length (meter)	2500.00	2500.00	2500.00	2500.00	2500.00	2500.00
6	In CR K > 38 (%)	35.35	29.12	28.21	28.75	24.73	18.50
7	In CR K > 28 (%)	38.46	32.23	35.53	30.95	29.85	23.26
8	In CR Avg. Speeds(km/hour) (%)	38.60	47.87	45.38	49.85	45.25	42.19
Scenario	**Features**	**Uncontrolled-% Change**	**LCS-% Change**	**VSL-% Change**	**Controlled-% Change**	**Predicted-% Change**	
0	K > 38%	-8.66	-10.59	-9.23	-21.56	-38.20	
1	K > 28(%)	-6.89	4.37	-10.85	-14.61	-25.31	
2	Overall Avg. K	-12.09	-8.36	-13.27	-13.11	-12.46	
3	Overall Avg. Speeds (km/hour)	24.02	22.39	26.80	25.44	22.87	
4	Shockwave duration (min)	22.50	22.50	22.50	22.50	22.50	
5	Shockwave length (meter)	2500.00	2500.00	2500.00	2500.00	2500.00	
6	In CR K > 38 (%)	-17.62	-20.21	-18.65	-30.05	-47.67	
7	In CR K > 28 (%)	-16.19	-7.62	-19.52	-22.38	-39.52	
8	In CR Avg. Speeds(km/hour) (%)	24.03	17.58	29.15	17.22	9.32	

Table 3.25. Scenario Control Distance=1250 Penetration Rate=70 Seed=4

Scenario	Features	Base	Uncontrolled	LCS	VSL	Controlled	Predicted
0	K > 38%	2.55	2.09	2.16	2.03	1.79	1.38
1	K > 28(%)	2.80	2.22	2.62	2.24	2.13	1.92
2	Overall Avg. K	11.59	9.48	9.60	9.47	9.70	9.40
3	Overall Avg. Speeds (km/hour)	61.52	80.95	80.16	80.79	78.93	79.28
4	Shockwave duration (min)	22.50	22.50	22.50	22.50	22.50	22.50
5	Shockwave length (meter)	2500.00	2500.00	2500.00	2500.00	2500.00	2500.00
6	In CR K > 38 (%)	35.35	26.19	27.11	25.27	22.34	15.75
7	In CR K > 28 (%)	38.46	28.02	33.33	28.02	26.74	20.51
8	In CR Avg. Speeds(km/hour) (%)	38.60	56.74	50.21	54.97	51.27	45.67
Scenario	**Features**	**Uncontrolled-% Change**	**LCS-% Change**	**VSL-% Change**	**Controlled-% Change**	**Predicted-% Change**	
0	K > 38%	-15.32	-20.45	-29.59	-45.87	-18.00	
1	K > 28(%)	-20.47	-6.32	-19.75	-23.67	-31.20	
2	Overall Avg. K	-18.19	-17.17	-18.28	-16.24	-18.89	
3	Overall Avg. Speeds (km/hour)	31.58	30.30	31.32	28.29	28.87	
4	Shockwave duration (min)	22.50	22.50	22.50	22.50	22.50	
5	Shockwave length (meter)	2500.00	2500.00	2500.00	2500.00	2500.00	
6	In CR K > 38 (%)	-25.91	-23.32	-28.50	-36.79	-55.44	
7	In CR K > 28 (%)	-27.14	-13.33	-27.14	-30.48	-46.67	
8	In CR Avg. Speeds(km/hour) (%)	47.02	30.08	42.43	32.83	18.33	

Results present in Table 3.24 are the results of the scenario, which is the optimum case for the unpredicted method. Comparing the results of the controlled and predicted controlled methods, it is easily observed that the predicted control method outperforms the controlled method at each density improvement-related parameter, but it is also seen that the controlled method has a better performance in speed improvements. Analyzing the results present in Table 3.25, which are the results of the optimum scenario for the controlled method, it is seen that SWSCAV [1] with the prediction again outperforms the controlled case at density improvements. On the other hand, checking the results present in Table 3.25, the predicted control method having higher percent decreases in density than the results present in Table 3.24 is an unexpected finding since Table 3.24 is constructed regarding the optimum case for the predicted control method. This unexpected event is due to the seed-applied because values in these tables are the results of two scenarios of one seed rather than being the average values of more seeds.

3.1.16. 3D Plots

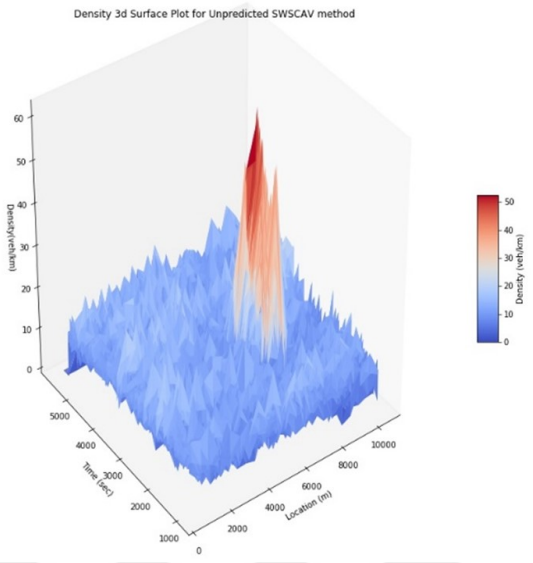

Figure 3.31. Density 3D Surface Plot for Controlled SWSCAV Method

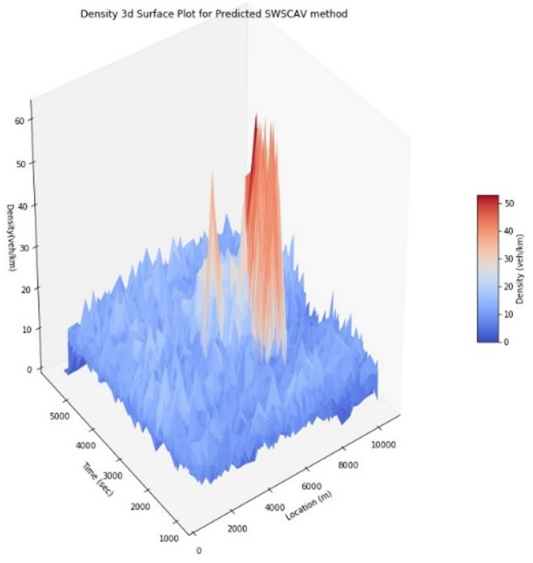

Figure 3.32. Density 3D Surface Plot for Predicted SWSCAV Method

Comparing the 3D plots present in Fig. 3.31 and 3.32, it is seen that there are more highly dense areas in the controlled method case. It is also observed that, at the predicted method case, density is distributed upstream to relieve the critical region. This distribution is related to the fact that the prediction tool added to the control method aims to predict the upstream boundary of the shockwave rather than using the current boundary of the shockwave. This makes the control distance start from a point, which is located more upstream. Therefore, at the predicted control method shockwaves are from farther away compared to the controlled method, which distributes the density as stated.

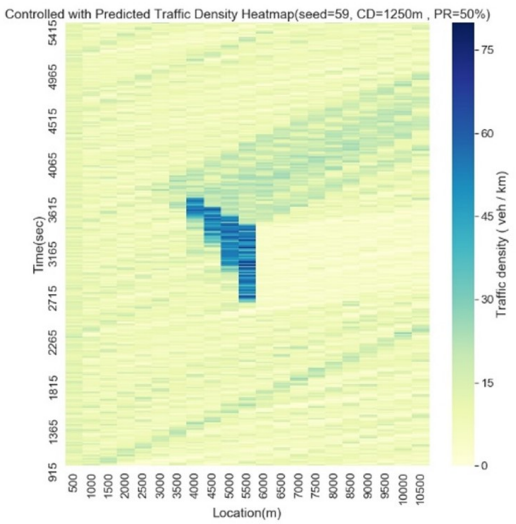

Figure 3.33. Controlled Traffic Density Heatmap(seed=59 CD=1250m PR=50%)

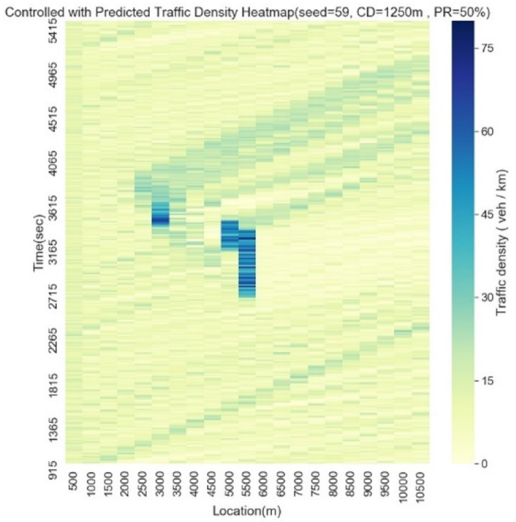

Figure 3.34. Predicted Traffic Density Heatmap(seed=59 CD=1250m PR=50%)

Heatmaps given in Fig 3.33 and 3.34, support the idea of the predicted control method starting the management of the shockwave from a farther point since in Fig. 3.34 there is a high-density zone created at a far spot and the highly-dense areas present in the critical region are mitigated. This improvement stabilizes the shockwave area by reducing the speed differences and reduces the stop-and-go motion of the vehicles present in the critical region.

4. CONCLUSION

In this thesis, SWSCAV [1], a real-time traffic management method using connected autonomous vehicles with and without prediction is tested and compared with LCS and VSL implementations. To achieve this, instantaneous or predicted sensor data were processed, and the speed and boundaries of the shockwave were determined. Afterward, the shockwave was transmitted to autonomous vehicles with speed-dependent to adjust their speed. SUMO simulation software was used to model and test the scenarios. SUMO is open-source microscopic simulation software. SUMO was chosen because TraCI, a TCP-based client-server architecture, allows the simulation to be manipulated with the Python 3.6 software language. A road network consisting of 11 kilometers and 3 lanes was created in the simulation environment. Performance criteria of these models are average density and speed values in the critical region. The critical region is defined as the smallest rectangle that contains the shockwave in a heatmap.

To test the performance of the real-time traffic management methods, a shockwave was created in the road network first. This shockwave is created by stopping a vehicle on the road in a random lane, in a random location, in a random period, and for a random time. The flow rate of the road network is 1500 veh / hour/lane. Within this flow, scenarios with 10%, 20%, 30%, 40%, 50%, 60%, 70% and 80% connected autonomous vehicles defined as penetration rate were created. Scenarios have been created in which this traffic flow value includes 10%, 20%, 30%, 40%, 50%, 60%, 70% and 80% connected autonomous vehicles. This ratio is called “penetration rate” through the thesis. Also, traffic management methods have variables. In the publication, which is a preliminary study of this thesis, variables giving the best results for VSL, and LCS were obtained. In the scenario where traffic is managed with instantaneous and predicted sensor data, control distances of 500, 750, 1000, 1250, and 1500 meters are chosen as the variable. 2400 scenarios were tested in 60 different scenario seeds, with 5 different control distances and 8 different penetration rates. During the simulation, when a shockwave is detected, the density and flow data collected from the sensors are firstly up-sampled with the Fast Fourier Transform algorithm to pre-

vent underutilization from the sensor opening. The up-sampled data are cleared from outlier values and smoothed with the Fused Lasso algorithm to determine important change points. Then, the shockwave speed at the upstream boundary of the shockwave is calculated and this value is transmitted to the connected autonomous vehicles to adjust their speed. In SWSCAV [1] with predicted sensor data, the only difference is that the density and flow values after 3 minutes are estimated before the sensor data is processed. The data is then processed by using those 3 minutes later density and flow data. This predicted density and flow data is formed as a result of estimating the heatmap of the last 2 minutes with Pix2Pix GAN algorithm. Pix2Pix Generative Adversarial Network or GAN is a deep learning algorithm designed to train the deep convolutional neural network to obtain an image from one image to another. Pix2Pix GAN algorithm has been trained with the neural network architecture that gives the best results, with 13125 input heatmap images and 13125 output images where shockwaves are observed. Each simulation takes 1.5 hours and a clear simulation of 1 hour is obtained by discarding the first and last 15 minutes.

It was observed that different variables of 2400 different scenarios affect the performance of the method differently. In the method in which instant traffic data is used, as the percentage of autonomous vehicles increases, the performance of the model gradually increases. Penetration rates of 70% and 80% give the best results. As the duration of the accident increased, the effectiveness of SWSCAV [1] implementation gradually decreased for each percentage of connected vehicles. At a 70% penetration rate, an average of 55.73% improvement was observed in short-duration accidents, while this rate decreased to 42.63% in long-duration accidents. SWSCAV [1] gives proportionally better results in traffic congestion covering less distance. In simulations, there was less queue in right lane accidents. Therefore, a proportionally higher improvement was observed in the right lane, while less improvement was observed in the middle and left lane than in the right lane. Besides, it is observed that as the control distance increases, both the average speed of the traffic increases and the density in the critical region decreases. In SWSCAV [1] implementation using instantaneous sensor data, the best improvement with an average improvement of 55.12% was observed at a 60% penetration rate and 1500 meters control distance. In SWSCAV [1] implementation with

predicted sensor data, the best results were obtained with 58.18% in scenarios with a 50% penetration rate. Except for 50% and 60% penetration rates, as in SWSCAV [1] implementation with instant traffic data, the proportional performance decreases as the duration of the accident increases. However, the penetration rate of 50% showed a more stable behavior compared to the other rates, showing improvements of 63.05%, 50.33%, and 59.24% in short, medium, and long-lasting accidents, respectively. In SWSCAV [1] implementation with predicted data, the improvement in traffic is similar in all lanes, unlike the method managed with instant data. Even at 70% and 80% penetration rates, there is a higher proportional improvement than in the right lane, where in the middle 54.9% and 49.75% and left lanes than in the right lane with 45.58% and 51.09%, respectively. In SWSCAV [1] with estimated data implementation, no significant improvement was observed in the penetration rates of 40% and above after 750 meters control distance. According to these results, the traffic can be managed with the highest efficiency with the requirement of lower control distance and penetration rate in studies conducted with estimated data.

In SWSCAV [1] implementation, the speed of the traffic flow is managed by using the information acquisition and implementation speeds of the connected autonomous vehicles. In this way, the regional density in traffic is reduced and a safer and more stable driving experience is aimed. Reducing the impact areas of accidents is important not only for the safety and driving experience but also for reducing the negative impact of traffic on the environment and community psychology.

The values found in this study may vary depending on many parameters such as traffic demand, road geometry, and driver aggressiveness. As further studies, subjects such as the speed given to vehicles different from the shockwave speed, a different data processing and transmission process, ideal traffic management with autonomous vehicle behavior in different road networks can be tested.

REFERENCES

1. Gokasar, I., A. Timurogullari and S. S. Ozkan, "Comprehensive Evaluation of the Effects of VSL and LCS Implementations with Connected Autonomous Vehicles", , 2020.

2. Dragan, I., P. Deveci and I. Gökaşar, "Prioritization of the Connected Autonomous Vehicles in Real-Time Traffic Management Implementations", *Sustainable Cities and Society*, 2021.

3. Avatefipour, O. and F. Sadry, "Traffic Management System Using IoT Technology - A Comparative Review", *2018 IEEE International Conference on Electro/Information Technology (EIT)*, p. 1041–1047, IEEE, May 2018.

4. Schulz, W., "Traffic management improvement by integrating modern communication systems", *IEEE Communications Magazine*, Vol. 34, No. 10, p. 56–60, Oct 1996.

5. Javaid, S., A. Sufian, S. Pervaiz and M. Tanveer, "Smart traffic management system using Internet of Things", *2018 20th International Conference on Advanced Communication Technology (ICACT)*, p. 393–398, IEEE, Feb 2018.

6. Barrero, F., S. Toral, M. Vargas, F. Cortés and J. Manuel Milla, "Internet in the development of future road traffic control systems", *Internet Research*, Vol. 20, No. 2, p. 154–168, Apr 2010.

7. Kim, G.-H., D.-S. Pae, W.-J. Ahn, K.-S. Ko, M.-T. Lim and T.-K. Kang, "Vehicle Positioning System using V2X that Combines V2V and V2I Communications", *IOP Conference Series: Materials Science and Engineering*, Vol. 922, p. 012009, Oct 2020.

8. Friedrich, B., *The Effect of Autonomous Vehicles on Traffic*, pp. 317–334, Springer

Berlin Heidelberg, Berlin, Heidelberg, 2016.

9. Talebpour, A. and H. S. Mahmassani, "Influence of connected and autonomous vehicles on traffic flow stability and throughput", *Transportation Research Part C: Emerging Technologies*, Vol. 71, p. 143–163, Oct 2016.

10. Ye, L. and T. Yamamoto, "Evaluating the impact of connected and autonomous vehicles on traffic safety", *Physica A: Statistical Mechanics and its Applications*, Vol. 526, p. 121009, Jul 2019.

11. Wu, C., A. M. Bayen and A. Mehta, "Stabilizing Traffic with Autonomous Vehicles", *2018 IEEE International Conference on Robotics and Automation (ICRA)*, p. 1–7, IEEE, May 2018.

12. Chang, Y. S., Y. J. Lee and S. S. B. Choi, "Is there more traffic congestion in larger cities? -Scaling analysis of the 101 largest U.S. urban centers-", *Transport Policy*, Vol. 59, p. 54–63, Oct 2017.

13. Ilgin Guler, S., M. Menendez and L. Meier, "Using connected vehicle technology to improve the efficiency of intersections", *Transportation Research Part C: Emerging Technologies*, Vol. 46, p. 121–131, Sep 2014.

14. Patel, R., M. W. Levin and S. D. Boyles, "Effects of Autonomous Vehicle Behavior on Arterial and Freeway Networks", *Transportation Research Record: Journal of the Transportation Research Board*, Vol. 2561, No. 1, p. 9–17, Jan 2016.

15. Luettel, T., M. Himmelsbach and H.-J. Wuensche, "Autonomous Ground Vehicles—Concepts and a Path to the Future", *Proceedings of the IEEE*, Vol. 100, No. Special Centennial Issue, p. 1831–1839, May 2012.

16. Davidson, P. and A. Spinoulas, "Autonomous Vehicles -What Could This Mean for The Future of Transport?", , 2015.

17. Fagnant, D. J. and K. Kockelman, "Preparing a nation for autonomous vehicles: opportunities, barriers and policy recommendations", *Transportation Research Part A: Policy and Practice*, Vol. 77, p. 167–181, Jul 2015.

18. Makridis, M., K. Mattas, B. Ciuffo, M. A. Raposo, T. Toledo and C. Thiel, "Connected and Automated Vehicles on a freeway scenario. Effect on traffic congestion and network capacity", , Apr 2018.

19. Olia, A., H. Abdelgawad, B. Abdulhai and S. N. Razavi, "Assessing the Potential Impacts of Connected Vehicles: Mobility, Environmental, and Safety Perspectives", *Journal of Intelligent Transportation Systems*, Vol. 20, No. 3, p. 229–243, May 2016.

20. Popescu, O., S. Sha-Mohammad, H. Abdel-Wahab, D. C. Popescu and S. El-Tawab, "Automatic Incident Detection in Intelligent Transportation Systems Using Aggregation of Traffic Parameters Collected Through V2I Communications", *IEEE Intelligent Transportation Systems Magazine*, Vol. 9, No. 2, p. 64–75, 2017.

21. Lee, J. and B. B. Park, "Evaluation of Variable Speed Limit under Connected Vehicle Environment", , 2013.

22. Olia, A., P. Izadpanah and S. Razavi, "Construction work Zone Traffic Management Using Connected Vehicle Systems", , 2012.

23. Khondaker, B. and L. Kattan, "Variable speed limit: A microscopic analysis in a connected vehicle environment", *Transportation Research Part C: Emerging Technologies*, Vol. 58, p. 146–159, Sep 2015.

24. Talebpour, A., H. S. Mahmassani and S. H. Hamdar, "Speed Harmonization: Evaluation of Effectiveness Under Congested Conditions", *Transportation Research Record: Journal of the Transportation Research Board*, Vol. 2391, No. 1, p. 69–79, Jan 2013.

25. Ramezani, H. and R. Benekohal, "Optimized Speed Harmonization with Connected Vehicles for Work Zones", *2015 IEEE 18th International Conference on Intelligent Transportation Systems*, p. 1081–1086, IEEE, Sep 2015.

26. Darroudi, A., "Variable Speed Limit Strategies to Reduce the Impacts of Traffic Flow Breakdown at Recurrent Freeway Bottlenecks", *FIU Electronic Theses and Dissertations*, Nov 2014.

27. Samimi Abianeh, A., M. Burris, A. Talebpour and K. Sinha, "The impacts of connected vehicle technology on network-wide traffic operation and fuel consumption under various incident scenarios", *Transportation Planning and Technology*, Vol. 43, No. 3, p. 293–312, Apr 2020.

28. Farrag, S. G., F. Outay, A. U.-H. Yasar, D. Janssens, B. Kochan and N. Jabeur, "Toward the improvement of traffic incident management systems using Car2X technologies", *Personal and Ubiquitous Computing*, Jan 2020.

29. Makridis, M., K. Mattas, B. Ciuffo, M. A. Raposo, T. Toledo and C. Thiel, "Connected and Automated Vehicles on a freeway scenario. Effect on traffic congestion and network capacity", , Apr 2018.

30. Kattan, L., M. Mousavi, B. Far, C. Harschnitz, A. Radmanesh and S. Saidi, "Microsimulation Evaluation of the Potential Impacts of Vehicle-to-Vehicle Communication (V2V) in Disseminating Warning Information under High Incident Occurrence Conditions", *International Journal of Intelligent Transportation Systems Research*, Vol. 10, No. 3, p. 137–147, Sep 2012.

31. Bauza, R., J. Gozalvez and J. Sanchez-Soriano, "Road traffic congestion detection through cooperative Vehicle-to-Vehicle communications", *IEEE Local Computer Network Conference*, pp. 606–612, 2010.

32. Hashmani, M., "Performance comparison and issues of congestion control schemes

in ATM networks", , 03 2021.

33. Wirtz, J. J., J. L. Schofer and D. F. Schulz, "Using Simulation to Test Traffic Incident Management Strategies: The Benefits of Preplanning", *Transportation Research Record: Journal of the Transportation Research Board*, Vol. 1923, No. 1, p. 82–90, Jan 2005.

34. Bauza, R. and J. Gozalvez, "Traffic congestion detection in large-scale scenarios using vehicle-to-vehicle communications", *Journal of Network and Computer Applications*, Vol. 36, No. 5, p. 1295–1307, Sep 2013.

35. Popescu, O., S. Sha-Mohammad, H. Abdel-Wahab, D. C. Popescu and S. El-Tawab, "Automatic Incident Detection in Intelligent Transportation Systems Using Aggregation of Traffic Parameters Collected Through V2I Communications", *IEEE Intelligent Transportation Systems Magazine*, Vol. 9, No. 2, p. 64–75, 2017.

36. Khan, Z., A. Koubaa and H. Farman, "Smart Route: Internet-of-Vehicles (IoV)-Based Congestion Detection and Avoidance (IoV-Based CDA) Using Rerouting Planning", *Applied Sciences*, Vol. 10, No. 13, p. 4541, Jun 2020.

37. Cárdenas-Benítez, N., R. Aquino-Santos, P. Magaña-Espinoza, J. Aguilar-Velazco, A. Edwards-Block and A. Medina Cass, "Traffic Congestion Detection System through Connected Vehicles and Big Data", *Sensors*, Vol. 16, No. 5, p. 599, Apr 2016.

38. Ta, V.-T. and A. Dvir, "A secure road traffic congestion detection and notification concept based on V2I communications", *Vehicular Communications*, Vol. 25, p. 100283, Oct 2020.

39. Guériau, M., R. Billot, N.-E. El Faouzi, J. Monteil, F. Armetta and S. Hassas, "How to assess the benefits of connected vehicles? A simulation framework for the design of cooperative traffic management strategies", *Transportation Research*

Part C: Emerging Technologies, Vol. 67, p. 266–279, Jun 2016.

40. Ghiasi, A., X. Li and J. Ma, "A mixed traffic speed harmonization model with connected autonomous vehicles", *Transportation Research Part C: Emerging Technologies*, Vol. 104, p. 210–233, Jul 2019.

41. Lee, J. and B. B. Park, "Evaluation of Variable Speed Limit under Connected Vehicle environment", *2013 International Conference on Connected Vehicles and Expo (ICCVE)*, pp. 966–967, 2013.

42. Erda, M., *Autonomous vehicles: Evaluation of traffic management strategies in the case of an incident*, Master's Thesis, Bogazici University, 2018.

43. Khattak, Z. H., B. L. Smith, H. Park and M. D. Fontaine, "Cooperative lane control application for fully connected and automated vehicles at multilane freeways", *Transportation Research Part C: Emerging Technologies*, Vol. 111, p. 294–317, Feb 2020.

44. Genders, W. and S. N. Razavi, "Impact of Connected Vehicle on Work Zone Network Safety through Dynamic Route Guidance", *Journal of Computing in Civil Engineering*, Vol. 30, No. 2, p. 04015020, Mar 2016.

45. Tajdari, F., C. Roncoli and M. Papageorgiou, "Feedback-Based Ramp Metering and Lane-Changing Control With Connected and Automated Vehicles", *IEEE Transactions on Intelligent Transportation Systems*, p. 1–13, 2020.

46. Zhou, M., X. Qu and S. Jin, "On the Impact of Cooperative Autonomous Vehicles in Improving Freeway Merging: A Modified Intelligent Driver Model-Based Approach", *IEEE Transactions on Intelligent Transportation Systems*, p. 1–7, 2016.

47. May, A. D., *Traffic flow fundamentals*, Prentice Hall, 1990.

48. Bailey, D. H. and P. N. Swarztrauber, "The Fractional Fourier Transform and

Applications", *SIAM Review*, Vol. 33, No. 3, p. 389–404, Sep 1991.

49. Tibshirani, R., M. Saunders, S. Rosset, J. Zhu and K. Knight, "Sparsity and smoothness via the fused lasso", *Journal of the Royal Statistical Society: Series B (Statistical Methodology)*, Vol. 67, No. 1, p. 91–108, Feb 2005.

50. Gökaşar, I., "Trafik Yönetiminde Şerit Kontrol Sistemlerinin Etkinliğinin İncelenmesi", *Teknik Dergi*, Vol. 27, No. 4, p. 7635–7657, 2016.